Kaunas University of Technology

Faculty of Mechanical Engineering and Design

Additive Manufacturing of Composite Structures using Biopolymers and Synthetic Fibres

Master's Final Degree Project

Tomas Simokaitis

Project author

Prof. Dr. Marius Rimašauskas

Supervisor

Kaunas, 2026

Kaunas University of Technology
Faculty of Mechanical Engineering and Design

Additive Manufacturing of Composite Structures using Biopolymers and Synthetic Fibres

Master's Final Degree Project

Industrial Engineering and Management (6211EX018)

Tomas Simokaitis
Project author

Prof. Dr. Marius Rimašauskas
Supervisor

Assist. Prof. Dr. Tomas Kuncius
Reviewer

Kaunas, 2026

Kaunas University of Technology

Faculty of Mechanical Engineering and Design

Tomas Simokaitis

Additive Manufacturing of Composite Structures using Biopolymers and Synthetic Fibres

Declaration of Academic Integrity

I confirm the following:

1. I have prepared the final degree project independently and honestly without any violations of the copyrights or other rights of others, following the provisions of the Law on Copyrights and Related Rights of the Republic of Lithuania, the Regulations on the Management and Transfer of Intellectual Property of Kaunas University of Technology (hereinafter – University) and the ethical requirements stipulated by the Code of Academic Ethics of the University;

2. All the data and research results provided in the final degree project are correct and obtained legally; none of the parts of this project are plagiarised from any printed or electronic sources; all the quotations and references provided in the text of the final degree project are indicated in the list of references;

3. I have not paid anyone any monetary funds for the final degree project or the parts thereof unless required by the law;

4. I understand that in the case of any discovery of the fact of dishonesty or violation of any rights of others, the academic penalties will be imposed on me under the procedure applied at the University; I will be expelled from the University and my final degree project can be submitted to the Office of the Ombudsperson for Academic Ethics and Procedures in the examination of a possible violation of academic ethics.

Tomas Simokaitis

Confirmed electronically

Kaunas University of Technology

Faculty of Mechanical Engineering and Design

Task of the Master's Final Degree Project

Given to the student – Tomas Simokaitis

1. Title of the Project

Additive Manufacturing of Composite Structures using Biopolymers and Synthetic Fibres

(In English)

Kompozicinių struktūrų adityvi gamyba naudojant biopolimerus ir sintetinius pluoštus

(In Lithuanian)

2. Aim and Tasks of the Project

Aim: to develop additively manufactured composite structures composed of biopolymers and synthetic fibres and investigate their mechanical properties.
Tasks:
1. to perform impregnation of synthetic fibres and determine its impact on the compatibility;
2. to prepare composite structure specimens by using material extrusion technology;
3. to evaluate reinforcement material content in a composite structure;
4. to determine the main mechanical properties of the composite structures and perform comparative analysis.

3. Main Requirements and Conditions

Composite structures must be composed of PHA or PHBH/PBS biopolymer matrices and reinforced with various types of synthetic fibres, such as carbon, glass, and aramid fibres.
Specimens should be prepared according to ASTM D3039 and ASTM D7264 standards.

4. Additional Requirements for the Project, Report and its Annexes

Not applicable

Project author	Tomas Simokaitis		04-02-2026
	(Name, Surname)	*(Signature)*	*(Date)*
Supervisor	Marius Rimašauskas		04-02-2026
	(Name, Surname)	*(Signature)*	*(Date)*
Head of study field programs	Regita Bendikienė		04-02-2026
	(Name, Surname)	*(Signature)*	*(Date)*

Simokaitis Tomas. Additive Manufacturing of Composite Structures using Biopolymers and Synthetic Fibres. Master's Final Degree Project, supervisor prof. dr. Marius Rimašauskas; Faculty of Mechanical Engineering and Design, Kaunas University of Technology.

Study field and area (study field group): Production and Manufacturing Engineering (E10), Engineering Sciences (E).

Keywords: composite structures; additive manufacturing; material extrusion; biopolymers; synthetic fibres.

Kaunas, 2026. 70 p.

Summary

This paper reviews AM technologies, their potential applications in composite structure manufacturing, and their capabilities and limitations. In addition, five MEX processes that can be used in the production of continuous fibre reinforced composite production are analysed. Moreover, towpreg preparation methods, which are used for CFRC production, and their benefits for composites are reviewed. Also, various types of biopolymers, their origins, advantages and disadvantages, and their potential applications in AM are discussed. The paper also describes the preparation process of synthetic towpregs, which were used in the additive manufacturing of composite structures. Continuous synthetic fibres were embedded with PHBH/PBS blend biopolymer matrix by applying the melt impregnation method, and the quality of the fibre impregnation was determined by the ASTM D4018 standard, which has shown that it is difficult to properly impregnate synthetic fibres with PHBH/PBS biopolymer and that each synthetic fibre type brings different processing challenges. Additionally, pull-out tests were conducted to determine the interfacial shear strength (IFSS) of synthetic fibres and biopolymers, as well as the effect of impregnation on IFSS, which showed that unimpregnated synthetic fibres are more compatible with the PHBH/PBS blend biopolymer than with the PHA matrix by 39%, and that synthetic fibre impregnation improves IFSS with biopolymers. Moreover, composite structures composed of PHA or PHBH/PBS blend biopolymers and synthetic fibres were additively manufactured by applying the towpreg co-extrusion method, in accordance with ASTM D3039 and ASTM D7264 standards. Tensile and flexural tests on these composite structures were performed, which results provided that these structures exhibit superior mechanical properties compared to pure biopolymers. Additionally, fibre, matrix, and air void content in a composite structure were determined in accordance with ASTM D2734 standard.

Simokaitis Tomas. Kompozicinių struktūrų adityvi gamyba naudojant biopolimerus ir sintetinius pluoštus. Magistro baigiamasis projektas, vadovas prof. dr. Marius Rimašauskas; Kauno technologijos universitetas, Mechanikos inžinerijos ir dizaino fakultetas.

Studijų kryptis ir sritis (studijų krypčių grupė): Gamybos inžinerija (E10), Inžinerijos mokslai (E).

Reikšminiai žodžiai: kompozitinės struktūros; adityvi gamyba; medžiagos ekstruzija; biopolimerai; sintetiniai pluoštai.

Kaunas, 2026. 70 p.

Santrauka

Šiame darbe apžvelgiamos adityvios gamybos (AG) technologijos, jų pritaikymo galimybės kompozicinių struktūrų gamyboje ir jų panaudojimo galimybės bei apribojimai. Be to, apžvelgiami penki medžiagos ekstrudavimo procesai, kurie gali būti naudojami kompozicinių struktūrų gamyboje, pritaikant ištisinius pluoštus armavimui. Taip pat aptariami pluoštų paruošimo metodai, kurie naudojami ištisinių pluoštų armuotų kompozitų gamybai, ir apžvelgta jų sutrekiama nuauda pritaikant juos kompozitų gamyboje. Be to, apžvelgiami įvairių tipų biopolimerai, jų kilmė, privalumai ir trūkumai bei galimos taikymo galimybės AG srityje. Darbe taip pat aprašomas sintetinių pluoštų paruošimo procesas, kuris buvo atliekamas prieš pritaikant pluoštus kompozicinių struktūrų adityvioje gamyboje. Ištisiniai sintetiniai pluoštai buvo impregnuoti PHBH/PBS mišinio biopolimerine matrica, pritaikant išlydyto impregnavimo metodą, o pluoštų impregnavimo kokybė įvertinta pagal ASTM D4018 standartą, kuris parodė, kad yra sudėtinga tinkamai impregnuoti vientisus sintetinius pluoštus PHBH/PBS biopolimeru ir kad kiekvienas sintetinio pluošto tipas kelia skirtingus apdorojimo iššūkius. Be to, buvo atlikti ištraukimo bandymai, siekiant nustatyti sintetinių pluoštų ir biopolimerų paviršių sąsajos stiprumą, taip pat impregnavimo daromą poveikį tarpusavio stiprumui. Bandymai parodė, kad neimpregnuoti sintetiniai pluoštai yra 39% labiau suderinami su PHBH/PBS mišinio biopolimeru nei su PHA matrica, ir kad sintetinių pluoštų impregnavimas pagerina adheziją su biopolimerais. Taip pat, kompozitinės struktūros, sudarytos iš PHA arba PHBH/PBS mišinio biopolimerų ir sintetinių pluoštų, buvo pagaminti adityviniu būdu, taikant impregnuoto pluošto koekstruzijos metodą pagal ASTM D3039 ir D7264 standartus, kurie taip pat buvo naudojami atliekant šių kompozicinių struktūrų tempimo ir lenkimo bandymus. Rezultatai parodė, kad šios kompozitinės struktūros pasižymi geresnėmis mechaninėmis savybėmis negu lyginant su grynais biopolimerais. Be to, pluošto, matricos ir oro ertmių kiekis kompozitinėje struktūroje buvo nustatytas pagal ASTM D2734 standartą.

Table of Contents

List of Figures

List of Tables

List of Abbreviations

AM – Additive Manufacturing;
MEX – Material Extrusion;
PMC – Polymer Matrix Composites;
CFRC – Continuous Fibre Reinforced Composites;
PLA – Polylactic Acid;
PHA – Polyhydroxyalkanoates;
DED – Direct Energy Deposition;
MJ – Material Jetting;
PBF – Powder Bed Fusion;
SL – Sheet Lamination;
VP – Vat Polymerization;
SLS – Selective Laser Sintering;
MJF – Multi Jet Fusion;
MMC – Metal Matrix Composites;
CMC – Ceramic Matrix Composites;
FDM – Fused Deposition Modeling;
DIW – Direct Ink Writing;
PET – Polyethylene Terephthalate;
ABS – Acrylonitrile Butadiene Styrene;
TPU – Thermoplastic Polyurethane;
PP – Polypropylene;
PA – Nylon;
PBF – Powder Bed Fusion;
DMLS – Direct Metal Laser Sintering;
SLM – Selective Laser Melting;
SLA – Stereolithography;
LCD – Liquid Crystal Display;
DLP – Digital Light Processing;
CLIP – Continuous Liquid Interface Production;
PCL – Poly(e-caprolactone);
PHB – Polyhydroxybutyrate;
PHBV – Poly(hydroxybutyrate cohydroxyvalerate);
PBS – Polybutylene Succinate;
PCL – Polycaprolactone;
PTT – Poly(trimethylene terephthalate);
PPP – Polypropylene;
PHBH – Poly(3-hydroxybutyrate-co-3-hydroxyhexanoate);
CF – Carbon Fibre;
GF – Glass Fibre;
AF – Aramid Fibre;
RC – Resin Content;
IFSS – Interfacial Shear Strength;
PEEK – Polyetheretherketone.

Introduction

Additive manufacturing (AM) technologies provide the opportunity to produce prototypes and final products with complex geometric shapes rapidly and flexibly, which is something that conventional manufacturing methods cannot achieve. According to the ISO/ASTM 52900:2021 standard, AM technologies are classified into seven different types of processes. One of these methods is material extrusion (MEX), in which materials are extruded through a nozzle [1, 2]. For MEX processes, often thermoplastic polymers are used as the main material to produce components. Therefore, this method can be applied to produce polymer matrix composites (PMC), where a thermoplastic polymer matrix is reinforced by synthetic or natural fibres in short or continuous fibre forms. There are five different MEX methods to produce continuous fibre reinforced composites (CFRC), where this type of composite structure is used in many various industry fields, since they provide possibilities to produce lightweight structures, which are characterised by having great mechanical properties, such as low density structures with high strength and stiffness [3]. Most consumers and governments seek and demand that products be as sustainable as possible, that they be made from natural or renewable sources, and that they be easy to recycle or reuse [4]. Traditional PMCs are commonly composed of thermoset resins, such as epoxy or polyester and are reinforced with synthetic fibres, such as carbon, glass, and aramid fibres. Therefore, these composites are unsustainable since they are produced from petroleum based materials and cannot be reused or recycled as easily as thermoplastic polymers. Also, during the production of these composites, a lot of waste is generated that cannot be reused. So, by using thermoplastic biopolymers as matrix material and applying AM technologies, there are possibilities to produce more sustainable composite structures, which could be used as an alternative to unsustainable traditional composites. Thermoplastic biopolymers such as biopolyesters provide a sustainable solution, because these materials are produced from renewable sources, including microbes and plants. Also, these materials are biodegradable, renewable, and non-toxic to people. For this reason, this type of polymer, such as polylactic acid (PLA) or polyhydroxyalkanoates (PHA), is used in the pharmaceutical, food, and biomedical industries [5]. Although these biopolymer materials have a positive impact on the environment, they usually have poorer mechanical properties compared to petroleum based thermoplastics. As a result, their use in structural products or elements is still limited. Moreover, it is shown that continuous fibres can improve the mechanical properties of thermoplastics components. However, only a few possible variations of composite structures have been researched on additively manufactured composite materials. Therefore, this study aims to develop and evaluate the mechanical properties of additively manufactured composites, which would be composed of biopolymers and synthetic fibres.

Aim: to develop additively manufactured composite structures composed of biopolymers and synthetic fibres and investigate their mechanical properties.
Tasks:
1. to perform impregnation of synthetic fibres and determine its impact on the compatibility;
2. to prepare composite structure specimens by using material extrusion technology;
3. to evaluate reinforcement material content in a composite structure;
4. to determine the main mechanical properties of the composite structures and perform comparative analysis.

Hypothesis: additively manufactured composite structures, composed of biopolymers and synthetic fibres are sustainable alternative to traditional composite structures.

1. AM Technologies, CFRC Production Methods, and Biopolymers Use in Additive Manufacturing

1.1. Additive Manufacturing Technologies

According to the ISO/ASTM 52900:2021 standard, there are seven different categories of AM technologies, which are applied to produce parts by adding materials layer by layer. This provides flexibility in design and the ability to achieve complex geometric shapes with a minimum amount of waste, which could be difficult to achieve by using traditional manufacturing processes such as milling or turning. These AM technologies are classified into binder jetting, direct energy deposition (DED), material extrusion (MEX), material jetting (MJ), powder bed fusion (PBF), sheet lamination (SL) and vat polymerization (VP). AM methods are selected by the materials used for these technologies or other factors such as the product's quality, size of the product and its application [6].

Many of these AM technologies can be applied to produce PMC, which can be classified into short or discontinuous, continuous fibre composites, and voxelated polymeric composites. Classification is based on the type of fibre and its composition in the composite structure. This type of composite structures commonly reinforced using synthetic or natural fibres. Both polymer matrix categories, which are thermoplastics and thermosets, are applied in the production of PMC by using AM technologies. Thermoplastics as raw materials are used in the form of filaments or powders, and are used accordingly in material extrusion, selective laser sintering (SLS) and multi jet fusion (MJF). Thermoset resins are commonly applied for the AM methods, which are MJ, MEX, and VP, where photopolymers and thermal curable resins are used [7]. It is also important to note that some AM technologies, such as powder bed fusion, can be applied in the production of metal matrix composites (MMC) and ceramic matrix composites (CMC) [8].

1.1.1. Binder Jetting

During the binder jetting process (Fig. 1.), parts are made by bonding powder particles together. Therefore it can work with almost any type of powdered material, which includes polymers, ceramics and metals, and in many cases, no heat sources are used during the process. Although this method makes it possible to produce large sized products quickly and without any additional supports, it still has the disadvantage of requiring post processing, which determines the final properties of the product, as the printed product is usually fragile. This binder jetting system works by firstly spreading a thin layer of powder supply using a powder spreading tool, then the print head jets the liquid binding agent in a desired pattern on the powder bed to form the desired layer, and lastly build platform lowers, where the next layer is going to be formed. After each layer, this process is repeated till part is produced [9].

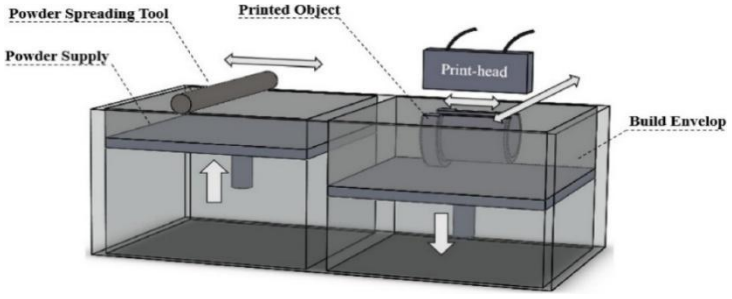

Fig. 1. Schematic of binder jetting process [9]

The binder jetting method can be applied to produce MMC, such as SiC-aluminium composites, by including SiC ceramic particles with an aluminium matrix. During production of SiC-aluminium composites, firstly SiC preforms get printed, then sintered, and only by using pressurised infiltration, mixed powder of aluminium and magnesium is added to the preform by merging SiC sintered preform into mixed powder and accomplishing infiltration process [10]. Since SiC ceramic material can be applied to binder jetting technology, it can also be applied to produce whisker reinforced CMC [11].

1.1.2. Direct Energy Deposition

The working principle of DED and deposition head is presented in Figure 2, where high density heat sources, such as lasers, electron beams, or plasma, are used to melt a substrate. Heat source forms the melt pool, where it melts deposited raw material, which can be in powder or wire form. Powdered metal material is usually inserted together with a carrier gas. As the deposition head moves forward together with heating source, deposited material solidifies on the substrate, leading clad tracks layer behind. Deposition head can be attached to 3-7 axis systems, which provides flexibility and precision for the process. This method commonly provides opportunities to use produce multi material components, large components, and it is also used for repair or coating purposes. For the DED process, various material classes are used, such as alloy and stainless steels, titanium, cobalt, nickel, aluminium, shape memory and high-entropy alloys, intermetallics, ceramics, composites, and functionally graded materials [12 – 15].

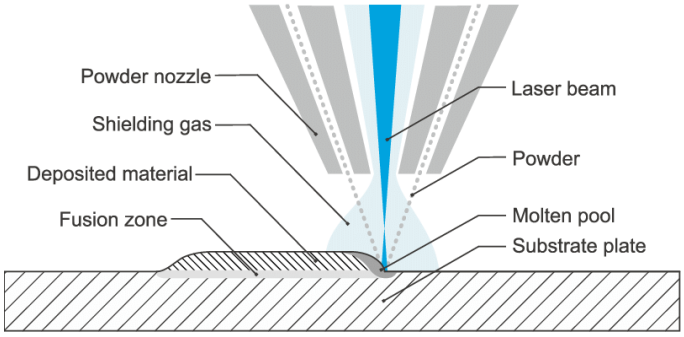

Fig. 2. Scheme of direct energy deposition process [16]

1.1.3. Material Extrusion

Material extrusion based AM technology is one of the most widely used methods, where materials are extruded through the nozzle or plunger on the print bed, where objects are printed (Fig. 3.). For this method, polymers, bio and food products, metals, ceramics and composite materials can be used in forms of liquefied solid, paste or gel. The main MEX technology, which is sometimes referred to as fused deposition modeling (FDM), is considered to be that which uses polymer thermoplastic material during the process, but MEX also includes robocasting or direct ink writing (DIW), where paste and gel type materials are used. Also, for this technology, metal and ceramic material extrusion is included, which requires additional processing steps in component production. For these processes, metal or ceramic powders are blended with thermoplastics to form extrudable material [17, 18].

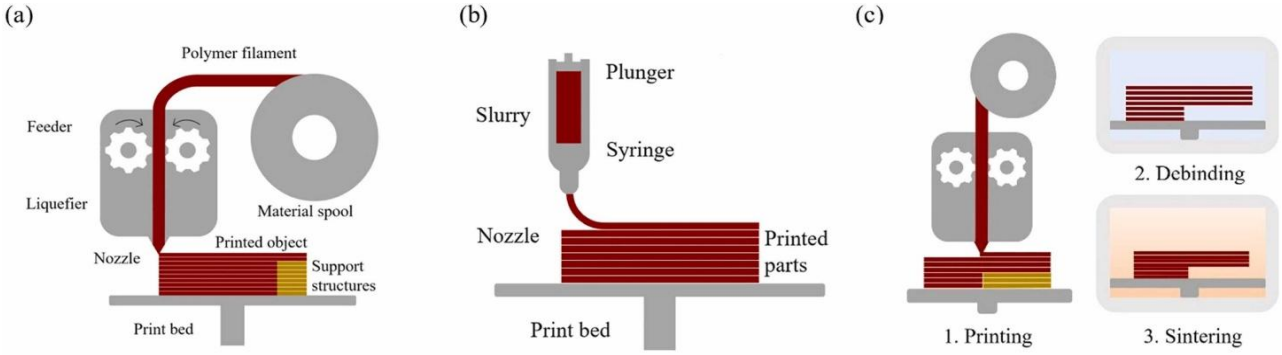

Fig. 3. MEX schematics: a) FDM, b) DIW, c) metal or ceramic extrusion [17]

For MEX, polymer matrix composites can be manufactured in various ways, and reinforcing fibres in the composite can be distributed not only in short or nanoparticle form, but also in the form of continuous fibre. Since this technology mainly uses thermoplastic polymer materials, such as PLA, polyethylene terephthalate (PET), acrylonitrile butadiene styrene (ABS), thermoplastic polyurethane (TPU), polypropylene (PP), and nylon (PA), which are relatively inexpensive materials that are easy and common to work with, but in some cases have insufficient mechanical properties. Therefore, these materials are being reinforced with discontinuous or continuous, synthetic or natural fibres to improve the mechanical properties of those matrixes. Discontinuous fibre reinforced composites are produced using modified filament, which is produced by mixing various short chopped fibres, whose length is commonly up to 100 µm, with matrix filament. To use modified filament, it is not necessary to use a specially modified extrusion head, and there are no restrictions on the geometric flexibility of the manufactured product when using this type of composite material. Meanwhile, in order to use continuous fibres to manufacture composite structures, it is necessary to use special extrusion heads and methods, and the possibility of producing products of a somewhat complex shape is reduced. However, polymer matrix continuous fibre reinforced composites have significantly better mechanical properties than composites reinforced with short fibres [19].

1.1.4. Material Jetting

In the material jetting process (Fig. 4.), photopolymers or jettable inks are deposited on build platform through the printhead as droplets, which form a thin layer of molten material, which is later cured using ultraviolet light emission. After each layer, build platform is lowered, and the process is repeated until the product is produced.

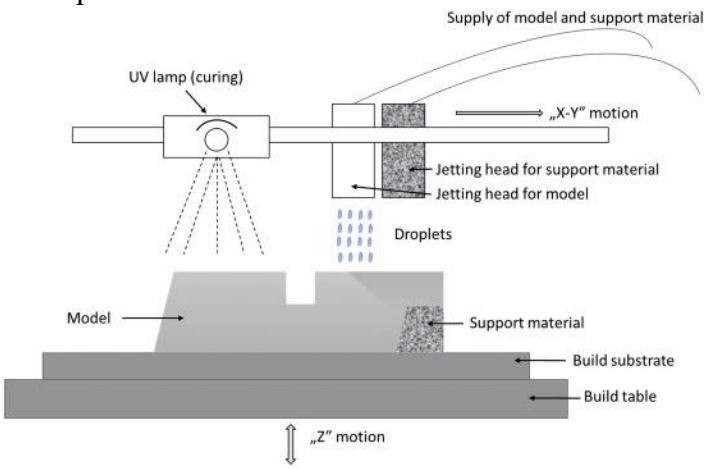

Fig. 4. Schematic of MJ technology [22]

This method allows to produce high quality parts with low surface roughness, since there is the possibility to produce thin layers, whose thickness can start from 16 µm. This technology also requires almost no additional post processing, only removal of supports, which are quite commonly used for this method since no overhang layer formation is possible using liquid materials. Supports are generated using different materials than building materials. One of the disadvantages of this method is the limited amount of available materials that can be applied to this method, and their poor mechanical properties. But still, MJ technology is being applied in the medical industry fields, in production of plastic injection moulds, and nanocomposites, where graphene, metal or ceramic fillers are used [20, 21].

1.1.5. Powder Bed Fusion

Powder bed fusion (PBF) technology (Fig. 5.) is somewhat similar to binder jetting. Here, instead of printing head, which spreads the binder, the heat source, such as a laser or electron bean is used to sinter or melt the powder material. This technology is classified into: selective laser sintering (SLS), direct metal laser sintering (DMLS), and selective laser melting (SLM) methods. For PBF printing various types of materials, including polymers, metals, and ceramics, in forms of a powder can be applied. Also, composite materials reinforced by nanoparticles are used. During the PBF process, for each layer, powder roller spreads powder stock onto the build platform, where particles are melted by using a heat source, which traces layer of the desired object shape. After each layer, steps are repeated till desired part is produced [23].

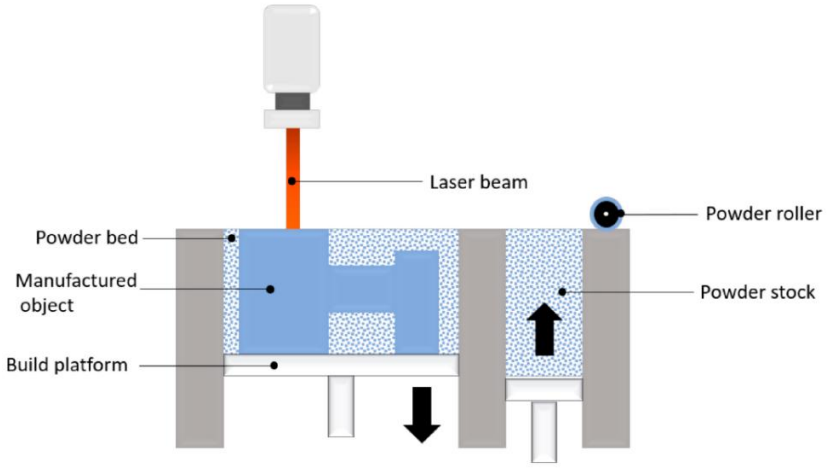

Fig. 5. Schematic of powder bed fusion technology [23]

Parts produced using PBF technology are usually characterized by having great surface finishes and mechanical properties. However, equipment and materials used for these methods are quite expensive and production time is quite consuming. This is one of the most widely used AM technologies in industry, which is adapted in aerospace and automotive industries, where lightweight and high strength with complex shape parts are required. Also, this processing method is often used in medicine, in the production of customized implants [24].

1.1.6. Sheet Lamination

Sheet lamination technique (Fig. 6.) is most unique AM technology, because products are manufactured by cutting and laminating material plates. For sheet lamination, the material must be in a sheet form that can be rolled, pressed and cut. Therefore, materials such as paper, polymer films or

composites, foils, ceramics, textiles and metal plates are used. Products are manufactured using this method by placing a layer of sheet on a platform. Then, by using a heated laminating roller, adhesives and pressure layers are joined together. Later layers outline and crosshatch of the product is typically cut out using a CO2 laser. Finally, the platform with part blocks gets lowered, and production steps are repeated till the final product is produced. Sheet lamination is no longer used so often because, during production, a large amount of waste is generated that cannot be reused, difficult post processing, and also more limitations on geometrical shapes compared to other AM technologies. This technique is mostly applied only for prototyping and sand casting tooling, due to the low material cost [25, 26].

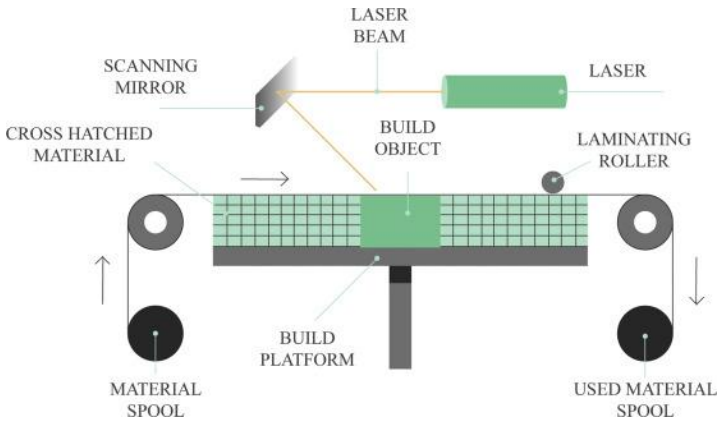

Fig. 6. Schematic of sheet lamination process [27]

1.1.7. Vat Polymerization

Vat polymerization is classified into many different techniques (Fig. 7.), such as stereolithography (SLA), liquid crystal display (LCD), digital light processing (DLP), and continuous liquid interface production (CLIP), which is somewhat similar to DLP. During any vat polymerization process, layer of liquid photosensitive resin material gets solidified in the desired shape by using a corresponding light source and wavelength. Different types of methods use different sources of light to harden the resin. In the SLA method, a laser is used as a light source, for the DLP projected light source is applied, and for the LCD array of ultraviolet light emitting diodes is applied [28, 29].

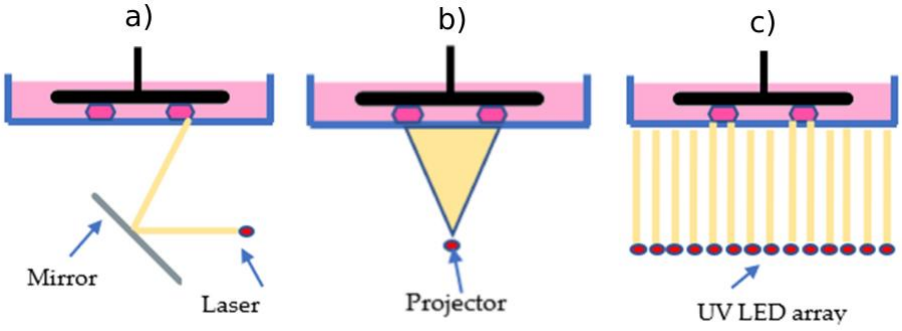

Fig. 7. Schematic of vat polymerization technologies: a)SLA, b)DLP, c)LCD [29]

Photopolymers that can be applied for vat photopolymerization commonly are classified into standard, structural, tough and durable, flexible and elastic, castable wax or ceramic, biocompatible, and bioink resins. All these raw material resins are selected differently according to the proposed mechanical and chemical characteristics. Therefore, because of materials variety and high precision

in parts dimensions, products, such as shoe soles, artificial ears, hearing aids, jewellery, microneedles, flexible electronics, smart composites, and many more complex components are being produced using these methods [30].

1.2. Continuous Fibre Reinforced Composites Production Methods

There are five methods to additively manufacture continuous fibre reinforced composites (CFRC) using MEX technology, which are classified as: towpreg extrusion, in-situ consolidation, in-line impregnation, in-situ impregnation, and towpreg co-extrusion (Fig. 8.).

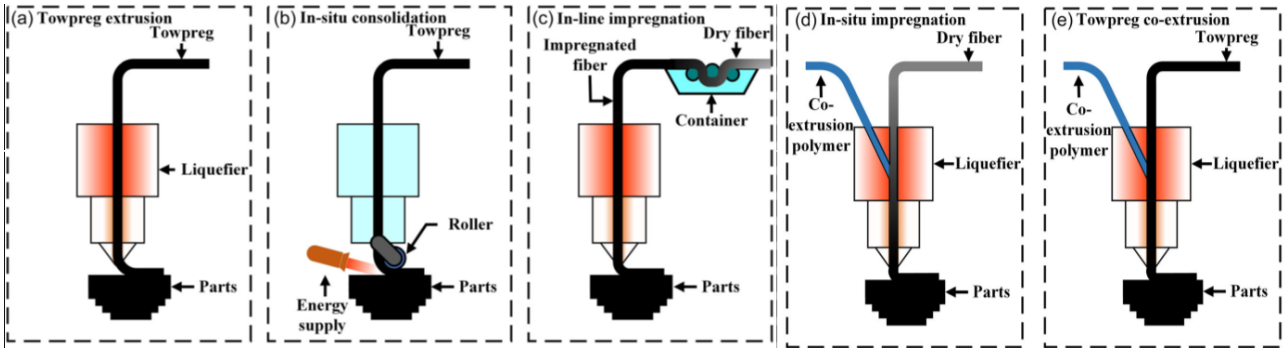

Fig. 8. Schematics of CFRC production methods [31]

These production methods of CFRC are proven to be highly promising. Since it provides the opportunity to produce customizable and complex shape products, which are characterized by having great mechanical properties with a high strength to weight ratio. Therefore, these composite structures, where thermoplastic matrixes are reinforced with continuous fibres, can be applied in various engineering applications, where lightweight components with high strength are required. Factors such as the content of the fibre within the composite or fibre volume fraction and fibre orientation impacts composites structures strength and stiffness. The larger the amount of fibre content in a composite structure, the greater mechanical properties composite would have. However, when additively manufacturing composites with high fibre content, problems as the following may arise: weak interfacial bonding, higher porosity, reduced printability, and material uniformity [31].

When applying MEX printing technologies for composites production, various types of printing heads are used. Processes are being divided according to their use into: single extrusion, in-situ co-extrusion, and dual extrusion (Fig. 9.). Single extrusion uses modified thermoplastic filaments, which are reinforced with additives in the form of nanoparticles or short fibres. Composite fibres consisting of continuous fibres and thermoplastic polymer can also be used in single extrusion. This method is called towpreg extrusion, where impregnated continuous fibre is extruded without additional matrix material. In both co-extrusion and dual extrusion, the matrix and continuous reinforcing fibres, are used separately and are joined only during printing, in the print head or directly on the printing platform or component. Dry or prepreg natural or synthetic fibres can be used during co-extrusion printing, commonly referred to as in-situ impregnation or towpreg co-extrusion. During double extrusion, the thermoplastic matrix and reinforcing fibres are extruded through separate nozzles, which allows the use of fibres only in certain places, where it is mostly needed [32].

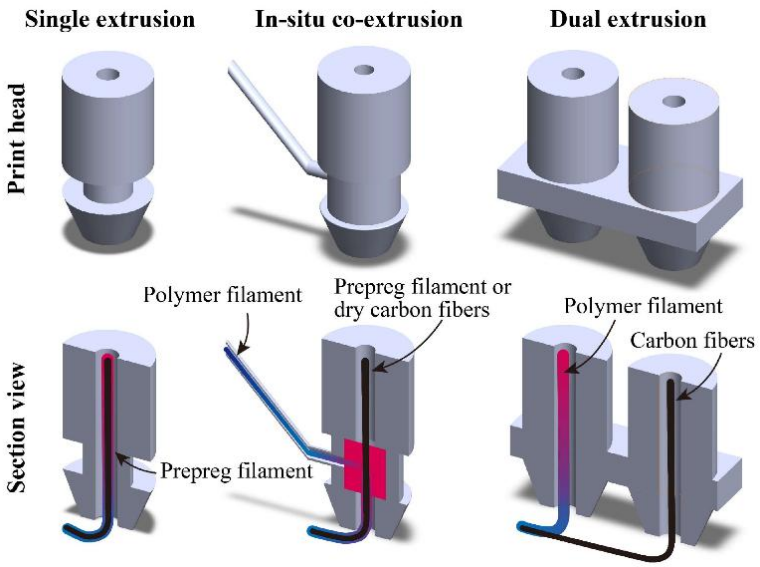

Fig. 9. Print head variations for composite production using MEX methods [32]

The least commonly used CFRC methods are in-line impregnation, where continuous dry fibres being impregnated during printing process, and in-situ consolidation, which is even contributed to automated fibre placement. The in-line impregnation method is very complicated and inefficient, as problems arising during impregnation directly affects the entire production line process. In-situ consolidation, such as other CFRC manufacturing methods provide possibility to produce high performance thermoplastic composite structures, during which production processes, continuous thermoplastic towpreg is layered on the build surface using a compaction roller and energy supply, such as a laser, which melts towpreg and helps to bond with other layers. Perhaps this method could be used in the manufacturing of aircraft thermoplastic composite components, but it is avoided due to such disadvantages as a complex process, which requires high demanding manufacturing equipment, capable of providing high temperature and pressure, which is needed to form high quality components using thermoplastic towpregs [33].

The more commonly in-situ impregnation and towpreg co-extrusion are used, because they provide more simplicity and flexibility in the production of CFRC. Both of these methods extrude a polymer matrix together with continuous reinforcing fibre. The only difference between them is that for in-situ impregnation, dry continuous fibres are used, and for towpreg co-extrusion already prepared towpreg is used. During in-situ impregnation, pure fibre tow is impregnated with thermoplastic matrix during the printing process, where the majority of printing settings drastically affect the mechanical properties of composite structures. The appropriate printing speed affects the quality of the fibre impregnation. When printing at higher speeds, the fibre tow gets poorer impregnation, which leads to voids in composite structures. Although the in-situ impregnation method is quite slow, it eliminates the need of pre impregnated fibre tow, which provides some cost reduction and flexibility [34, 35]. The towpreg co-extrusion method has somewhat similar advantages and disadvantages to in-situ impregnation, but when using already prepared continuous towpreg for composites production, bonding between matrix material and reinforcing fibre in order to improve printing quality, and also to make the printing process less complicated [36 – 39].

Continuous reinforcing fibres for MEX processes are prepared or impregnated in order to bond individual fibres of fibre tows bundles and increase their compatibility with the matrix thermoplastic used for printing processes. Towpregs for production processes are prepared accordingly to the type

of CFRC printing method that they are going to be used in. Fibres before production can be processed by applying conversional solution infiltration technologies or by coating the fibres with thermoplastic or thermoset resin, which is usually the same or similar material to the matrix material used for composite structure, and also it is referred to as melt impregnation. During conversional solution infiltration fibres usually impregnated by pulling them through a mixture of dissolved thermoplastic, which is dissolved in a selected solvent. This impregnation method can be simpler in some cases, as the dissolved substance used is less viscous and can be more easily absorbed into the fibre. However, most solvents are toxic, making this process harmful, and solvents could even damage the properties of the matrix or fibre materials. These disadvantages can be avoided by applying the melt impregnation method, in which no additives are used. During this impregnation method fibres are pulled through melted thermoplastic material, which is melted in the container with the help of an extruder. After coating the fibre with thermoplastic, the desired towpregs diameter is achieved by selecting the appropriate output nozzle of the container [40 – 45].

1.3. Biopolymers and Their Use in Additive Manufacturing

Biopolymers are materials that are produced from natural or plant-based resources, including biowastes or crops. These materials are characterised by the fact that they are biodegradable and can be broken down in natural environments, into biomass, water, carbon dioxide, and organic macromolecular materials. Also, biopolymers are known for their cost efficiency, biodegradability, renewability, and other environmentally friendly factors, such as non-toxicity and ease of extraction [46]. Biopolymers are classified according to where they have been derived, commonly into polysaccharides, protein derived polymers, and biopolyesters. Polysaccharides are commonly derived from plants, such as cellulose, hemicellulose, lignin, pectin, alginate, and starch. Protein derived polymers can be derived from animals and plants, and these types of polymers are extracted from functional amino acid groups, such as wheat protein, soy protein, sunflower protein, gelatine, collagen and gluten. Deriving protein-derived polymers is a difficult process, and these types of polymers have poor mechanical properties and high moisture sensitivity. A group of biopolyesters is produced from plants and microbes. This group includes PLA, PHA, poly(e-caprolactone) (PCL), and many more polymers [47]. For example, biopolyesters such as PHA, poly(hydroxybutyrate) (PHB), poly(hydroxybutyrate cohydroxyvalerate) (PHBV), and other similar copolymers are fermented from microorganisms. While PLA, polybutylene succinate (PBS), polycaprolactone (PCL), poly(trimethylene terephthalate) (PTT), polypropylene (PPP), and other types of homo-polyesters, aliphatic co-polyesters, and aromatic co-polyesters are produced from biotechnology via conventional synthesis methods. Most of the mentioned materials can be applied in additive manufacturing, as long as they can be extruded and classified as thermoplastic [48]. Not only biopolyesters, but also agro-polymers, specifically starches, can be applied in additive manufacturing. However, there have been only a few attempts to produce starch-based products [49].

Different biopolyesters are characterised by different mechanical and processing properties, as well as biodegradability. Some studies examining the degradation of biopolymers have found that biopolyesters produced from microorganisms, such as PHB and poly(3-hydroxybutyrate-co-3-hydroxyhexanoate) (PHBH), are characterised by having better decomposition in soil than biopolymers produced from biotechnology, such as PLA and PBS. PHA in soil with food wastes could lose approximately 14.1%, and PHBH about 18.8% of their mass in 4 months. In the same

conditions and time period, PLA would not lose any weight, and PBS would lose only of 1.2% their mass [50].

Most commonly used biopolymer in AM is PLA, because of its quite good mechanical properties, desired thermal properties and processing ease. Other materials, including PCL or PHA, which bring different processing properties, can be applied in AM and used for MEX or PBF methods. PCL material in AM is applied for the production of implantable medical devices, since it is suitable for applications where long degradation times are required, and can be degraded in the human body initially through hydrolysis of the ester bonds. Recently, there has been a growing trend toward using PHA material. However, this material is characterised by having a lower glass transition temperature than PLA, which makes this material exhibit poorer physical properties and makes it less suitable for AM processes. In order to improve its processability and ductility, PHAs copolymer groups, such as PHB, PHBV and PHBH, are developed and used. From all PHA groups copolymers, PHBH provides a wider processing window, better thermal stability, and mechanical characteristics, making it suitable for applications where flexibility and compostability are needed [51, 52].

1.4. Chapter Summary

This chapter reviews seven main AM technologies and their potential applications in composite structure manufacturing, as well as their capabilities and limitations. In addition, five MEX processes that can be used in the production of continuous fibre reinforced composite production are reviewed. Also, towpreg preparation methods, which are used for CFRC production, and their benefits for composites are discussed. This section also describes various types of biopolymers, their origins, advantages and disadvantages, and their potential applications in AM. Furthermore, there is an increasing interest and high demand for sustainable manufacturing methods and renewable or recyclable materials in the production of composite structures. Moreover, there is a lack of research on these types of additively manufactured continuous fibers reinforced composites, where biopolymers are applied. Most of the studies and industrial applications are focused on petroleum based polymers and traditional composite manufacturing methods, which provide great mechanical properties but are highly unsustainable. Therefore, further research is needed to develop more sustainable composite structures that could replace traditional, unsustainable composite materials.

2. Methodology

2.1. Materials

For this project, two different types of biopolymers are used: PHA and a PHBH/PBS blend with a ratio of 50%/50% in the form of filament, which both of them have a diameter of approximately 1.75 mm. Both of these materials have a similar appearance but differ in their mechanical and processing properties. Mechanical properties of pure PHA, PHBH, and PBS biopolymers are provided in Table 1. PHA polymer has a density of approximately 1.24 g/cm^3 and has a low melting temperature, which is 140-170 °C, and also this material has a low glass transition temperature [53]. PHBH is a copolymer of PHA, with similar properties, which has a density of 1.24 g/cm^3, and whose melting temperature is 150-190 °C [52]. PBS thermoplastic is quite a flexible material, and it has a density of 1.25 g/cm^3, a melting temperature point of 90-120 °C, and this material has a low glass transition temperature, which ranges from -45 to -10 °C [57]. PHA is classified as having a high crystalline nature, which makes it difficult to thermally process this material. Therefore, PBS is introduced to PHBH, and a PHBH/PBS blend filament is produced to decrease crystallinity.

Table 1. Mechanical properties of pure PHA, PHBH, and PBS biopolymers

Material and references	Tensile strength, MPa	Young's modulus, MPa	Bending strength, MPa	Flexural modulus, MPa
PHA [53, 54]	19.0-20.2	104.3-540	29.3	1000
PHBH [55, 56]	13-23	200-1267	29.5	1029
PBS [58, 59]	35-37.8	675.2	21.4	613.2

These matrixes in composite production were reinforced with synthetic fibres, such as 3K carbon (CF), e-glass (GF), and aramid (AF) fibres (Fig. 11.). Also fibre impregnations with PHBH/PBS were carried out before applying them in AM processes, and other tests were conducted on them to determine their compatibility with biopolymers, the consistency of the impregnation, and the fibre content in the composites.

a b c

Fig. 10. Synthetic fibre tows: a – 3K carbon fibre, b – glass fibre, c – aramid fibre

Mechanical properties of these synthetic fibres are provided in Table 2. Carbon fibre is characterised by having a significantly higher stiffness compared to other synthetic fibres. Glass fibre has a higher density and lower strength, but it is more flexible and less brittle. Aramid offers lower density than other fibres, and also it has similar properties to glass fibre, but it is more expensive.

Table 2. Mechanical properties of synthetic fibres [60 – 62]

Synthetic fibres	**3K Carbon fibre**	**E-glass fibre**	**Aramid fibre**
Density g/cm3	1.8	2.55	1.44
Tensile strength, MPa	4230	2650	2950
Tensile modulus, GPa	254	72	91
Elongation at break, %	1.6	4.5	3.6

2.2. Melt Impregnation of Continuous Synthetic Fibres

The impregnation of synthetic fibres with PHBH/PBS blend biopolymer is performed to improve the mechanical properties of manufactured composites and to ensure better bonding between the matrix and reinforcing material [63]. During melt impregnation (Fig. 11.), an unimpregnated synthetic fibre (1) is pulled through a melted PHBH/PBS blend polymer (2), which is fed into a heating block through an extruder (3), where in the inner chamber the molten biopolymer impregnates the continuous fibre tow. Then the towpreg is cooled down by a fan (4) and wound onto a spool (5), which is driven by a stepper motor. The temperature of the heating block is set to 190 °C, the PHBH/PBS filament is fed into the heating block at a speed of 12 mm/min, and the stepper motor, which is pulling the fibres, rotates at a speed of 4 RPM, which is equivalent to approximately 1200 mm/min linear speed.

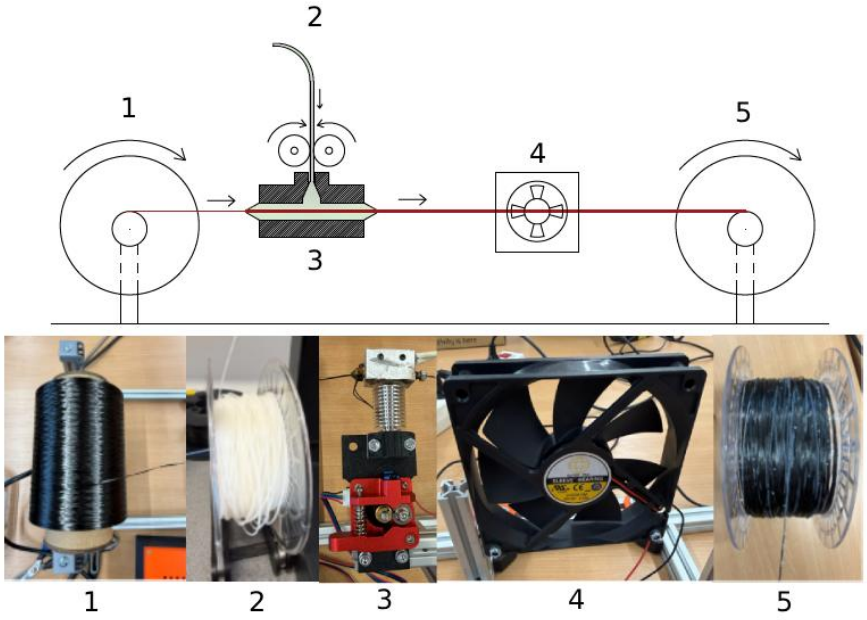

Fig. 11. Scheme of melt impregnation method

Unimpregnated fibre is fed into the heating block through the input nozzle, and impregnated towpreg is fed out through the output nozzle. These are interchangeable nozzles, and by using different diameter nozzles, it is possible to control the diameter of the impregnated fibre and the amount of

coating polymer matrix. For this study, a 1.5 mm diameter input nozzle and a 0.8 mm output nozzle were chosen based on experimental work.

2.3. Resin Content of Towpregs

After impregnation of synthetic fibres, it is important to assess the quality of the impregnation and calculate the amount of matrix that has penetrated the fibre tow, which is determined by resin content (RC) and can be calculated according to ASTM D4018 standard [64]. According to this standard, towpreg should be uniformly impregnated and should contain 35 to 60% of resin by weight. Resin content of impregnated fibre calculated using following equation:

$$RC = 100(1 - (MUL/MUL_i)) \quad (1)$$

where RC – resin content, %; MUL – mass per unit length of fibre, g/m; MUL_i – mass per unit length of impregnated fibre, g/m. Mass per unit length calculated using following equation:

$$MUL = W_1/L \quad (2)$$

where MUL – mass per unit length, g/m; W_1 – mass of the specimen, g; L – length of specimen, m. For these measurements, unimpregnated 3K CF, GF, and AF, and the same synthetic fibres impregnated with PHBH/PBS blend biopolymer were used as specimens. In total, 6 groups of 10 specimens in each group were prepared. Specimens were prepared by chopping fibre tows to 1 m (± 0.02 mm) in accordance with ASTM D4018 standard, and then they were weighed using "KERN ADJ 200-4" analytical scales (Fig. 12.) with 0.0001 g measurement readability and ±0.0004 g linearity.

Fig. 12. Fibre tow weighing using analytical scales

2.4. Interfacial Shear Strength Determination Between Synthetic Fibres and Biopolymers

Interfacial shear strength (IFSS) determines the resistance of the interface between the matrix and fibre materials. To evaluate the compatibility of synthetic fibres and biopolymers and determine the

effect of impregnation on adhesion, the multiple-fibre pull-out test is conducted [65 – 68]. In total, 12 groups of 10 specimens for each group were prepared. The selected classification of groups based on the materials used is shown in Table 3.

Table 3. Classification of IFSS specimens

Fibre types		**Matrixes**	
		PHA	**PHBH/PBS**
Unimpregnated	Carbon fibre	PHA/CFn	(PHBH/PBS)/CFn
	Glass fibre	PHA/GFn	(PHBH/PBS)/GFn
	Aramid fibre	PHA/AFn	(PHBH/PBS)/AFn
Melt impregnated with PHBH/PBS	Carbon fibre	PHA/CFm	(PHBH/PBS)/CFm
	Glass fibre	PHA/GFm	(PHBH/PBS)/GFm
	Aramid fibre	PHA/AFm	(PHBH/PBS)/AFm

All of the specimens were prepared by melting PHA or PHBH/PBS blend pellets around the unimpregnated or melt impregnated synthetic fibres. For all types of specimens, 0.3 g of matrix material for each specimen is used, except for PHA/CFn, PHA/GFn, and PHA/AFn groups. For these groups, 0.25 g of PHA is selected. To weigh matrix pellets, "BLOW JS13" scales with ±0.01 g measurement accuracy were used. Weighted matrix pellets placed in a cylindrical form casting mould with continuous synthetic fibre (Fig. 13.). Prepared casting mould with matrix material and fibres placed in „Memmert" oven. For specimens with PHA matrix material, the mould is placed in an oven preheated to 180 °C, and the specimens are heated for 25 minutes until pellets have completely melted and coated synthetic fibre tow. Specimens with PHBH/PBS blend matrix were placed in an oven at 195 °C for 40 minutes.

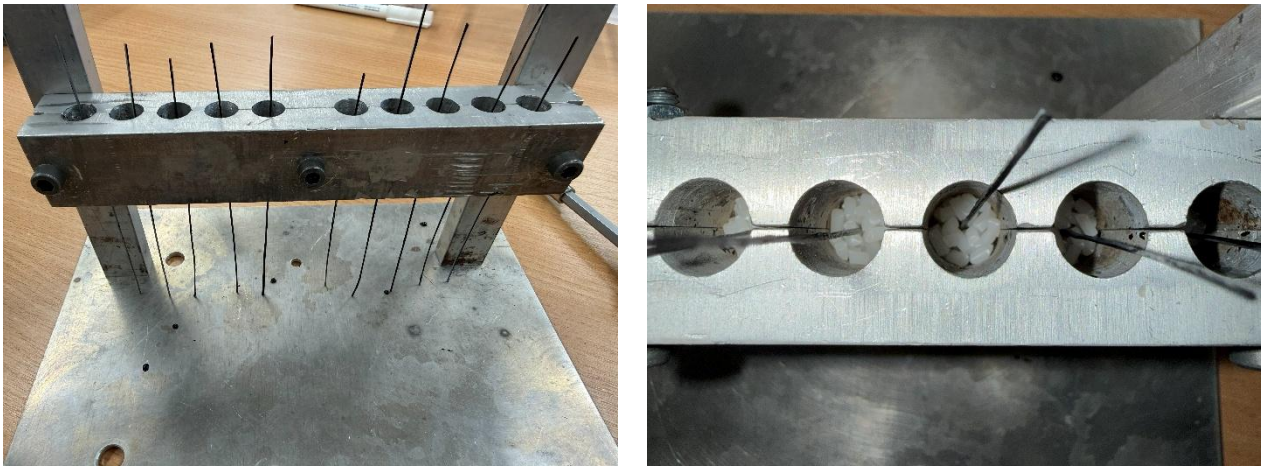

a b

Fig. 13. Prepared casting mould for IFSS specimens production: a – side view, b – top view

After removing the casting mould form with specimens from the oven. It was left to cool down at room temperature for 2 hours, so the mould could cool down completely and the polymer matrix could crystallise. Then the specimens were removed from the mould and prepared for IFSS testing. Before accomplishing pull-out testing, the formed matrix plate thickness and embedded fibre tow length (Fig. 14 b.) were measured with a ±0.01 mm accuracy calliper. Also, before the test, tabs were attached to the fibre ends. These tabs were placed in the tensile grips of the testing machine during

pull-out testing. Adhesion forces were determined by applying the fibre pull-out test method on prepared IFSS test specimens. To perform these tests, the "Tinius Olsen M25KT" universal mechanical testing machine is used. The IFSS specimen fibre is clamped by machine grips, and the matrix plate is placed behind the fixture plate (Fig. 14 a.). During pull-out testing, the matrix plate is held in place, and the fibre is pulled out at a 2 mm/min speed till synthetic fibre tow is pulled out of the matrix material.

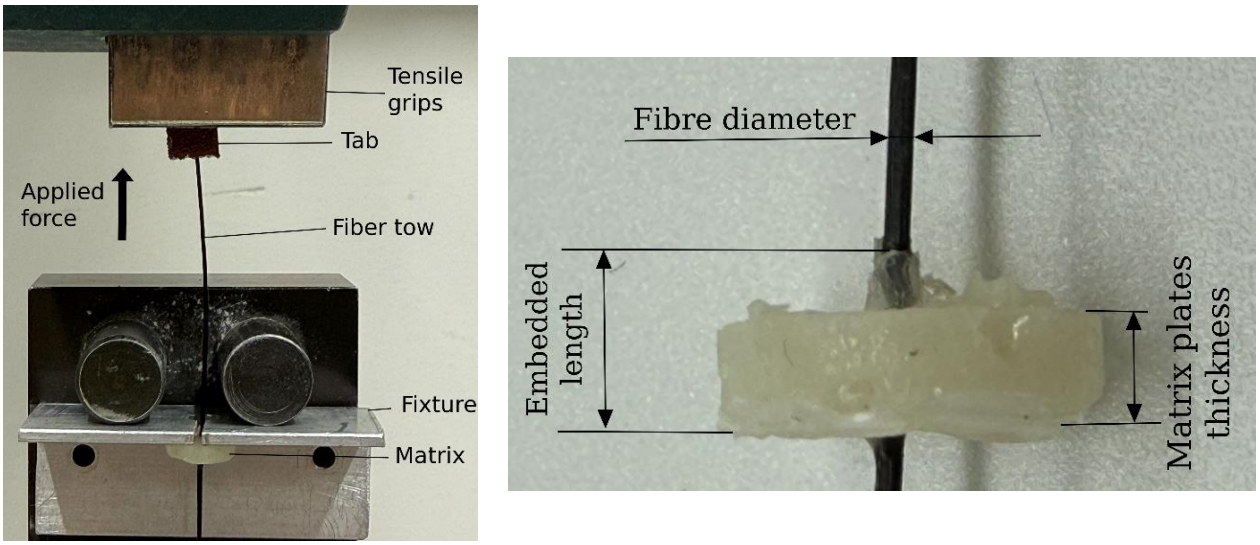

a b

Fig. 14. Interfacial shear strength: a – pull-out testing scheme, b – specimen dimensions

During IFSS pull-out testing, only force and displacement are obtained. For IFSS calculation, it is required to know the maximum force, which is required to pull out the fibre from the matrix plate, the embedded fibres length of the specimens, which was measured before testing, and fibres diameter. IFSS is calculated according to the following formula:

$$\tau_{IFSS} = \frac{F}{\pi \mathrm{dL}} \tag{3}$$

where τ_{IFSS} – interfacial shear strength, MPa; F – maximum force required to pull-out fibre tow, N; d – fibre tow diameter, mm; L – embedded fibres length, mm. Since fibre tow diameter cannot be measured using measuring instruments such as a calliper or micrometre. Therefore, the diameter has been calculated by fibre tow cross-sectional area using an analytical method. It is known that the theoretical 3K CF tow cross-sectional area is 0.12 mm^2 [69]. GF tow weight/length ratio is 0.3 g/m, and its density is 2.55 g/cm^3, which makes its cross-sectional area similar to that of 3K CF fibre tows. The weight/length of the used aramid fibre tow ratio is 0.09 g/m, and its density is 1.44 g/cm^3 [62]. Therefore, its cross-sectional area is 0.063 mm^2. Glass and aramid fibre tow cross-sectional areas were calculated by dividing the weight/length ratio by linear density. These cross-sectional areas were calculated to diameter, using the following formula:

$$d = \sqrt{\frac{4A}{\pi}} \tag{4}$$

where d – synthetic fibre tows diameter, mm; A – cross-sectional area of the synthetic fibre tow, mm^2. Calculated 3K CF and GF tows diameter is 0.39 mm, and AF diameter is 0.28 mm.

2.5. Composites Additive Manufacturing

For the production of composite specimens, which were used for tensile and flexural tests, a modified MEX printer "GeeeTech MeCreator 2" (Fig. 15.), with a custom designed towpreg co-extrusion head is used. This custom heating head is designed to produce composite structures, and this printer has a build volume of 160x160x160 mm.

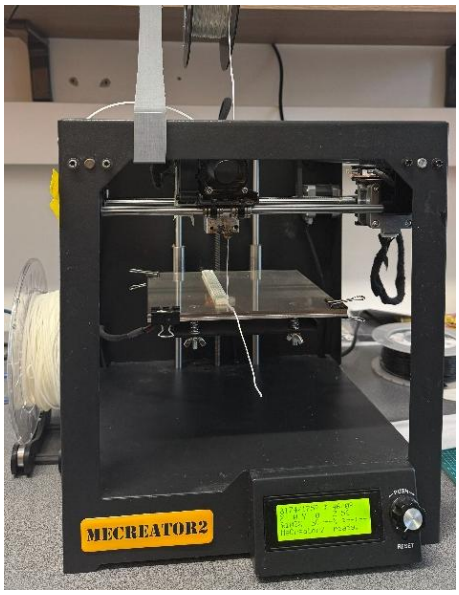

Fig. 15. "GeeeTech MeCreator 2" printer

A special towpreg co-extrusion print head (Fig. 16.) is designed to combine thermoplastic materials with the prepared continuous reinforcing fibres during the printing process. Towpregs are deposited on the printing bed by the traction force, which occurs when the deposited polymer solidifies and holds fibre on the print bed or part, and the head moves forward. The inner diameter of the used nozzle was 1.5 mm.

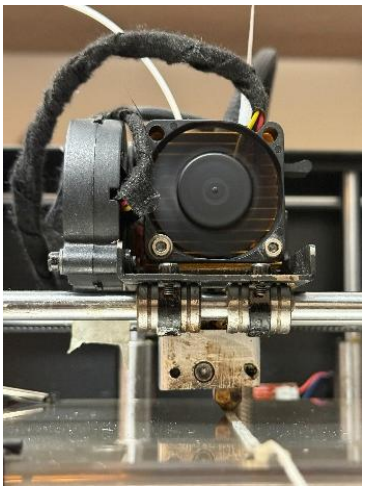

a

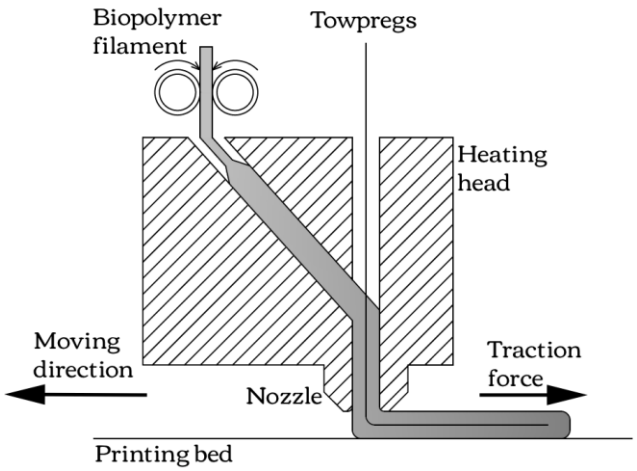

b

Fig. 16. Towpreg co-extrusion head: a – during the printing process, b – scheme

For this study, tensile and bending test specimens were additively manufactured in accordance with ASTM D3039 and ASTM D7264 standards, which are standard test methods for tensile and flexural properties of polymer matrix composite materials [70, 71]. Before manufacturing specimens, model

files of different sizes were designed using “SolidWorks” 3D modelling software, and based on these models, processing paths were generated, and other printing parameters were chosen using “Simplify 3D” slicing software. A model with a rectangular cross-section of 150x13.2x0.8 mm is designed for tensile specimens, and a model with a rectangular cross-section of 150x13.2x4 mm is designed for flexural specimens. Accordingly, the printing parameters listed in Table 4 were selected based on the intended use of the specimen and the matrix material used.

Table 4. Printing parameters for composite specimens

Parameters	**Tensile specimens**		**Flexural specimens**	
	PHA	**PHBH/PBS**	**PHA**	**PHBH/PBS**
Layer height	0.4 mm		0.5 mm	
Extrusion width	1 mm		1.2 mm	
Extrusion multiplier	0.75		0.6	
Extruder temperature	170 °C	185 °C	170 °C	175 °C
Print bed temperature	30 °C	55 °C	30 °C	50 °C
Movement speed	180 mm/min			

The parameters were selected experimentally, layer height and extrusion width selected so that the tensile specimen would consist of 2 printed layers and 11 unidirectional lines, and flexural specimens would consist of 8 printed layers and 9 unidirectional lines (Fig. 17.). The extrusion multiplier value of filament is selected less than 1, because at the extrusion time, matrix material is fed together with towpreg. This value is selected to ensure that neither too much nor too little matrix material is extruded during printing. These parameters influence the mechanical properties of the composite specimen, as their selection determines the amount of reinforcing fibres and air voids in the composite structure.

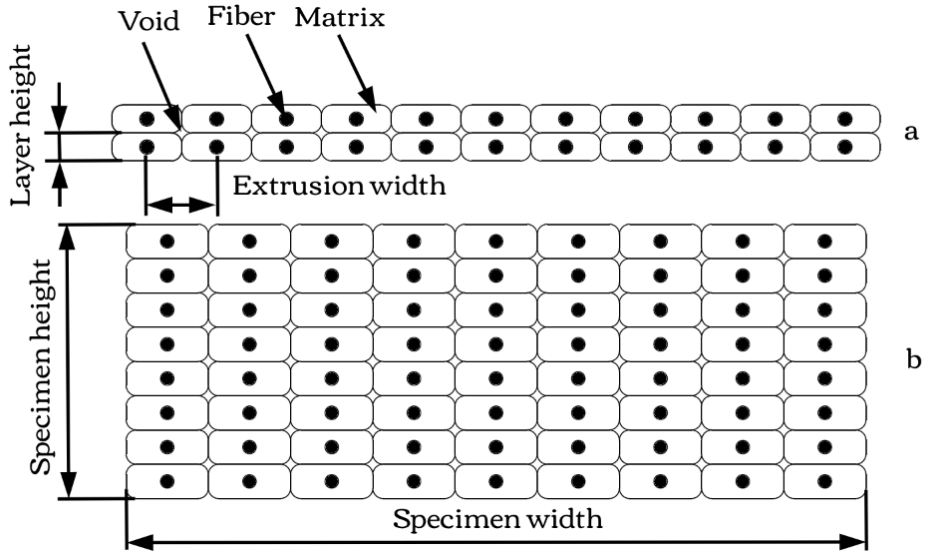

Fig. 17. Cross-sectional view of composite specimens: a – tensile specimen, b – flexural specimen

The generated print path (Fig. 18.) is a continuous path with no deviations, meaning that each new layer starts at the same positioning, shifting only by the layer height. In order to maximise the tensile

strength of the specimen, all fibres in the composite are aligned in a single direction and parallel to the loading direction, so that the reinforcing efficiency, as determined by Krenchel's factor, is equal to 1 [72].

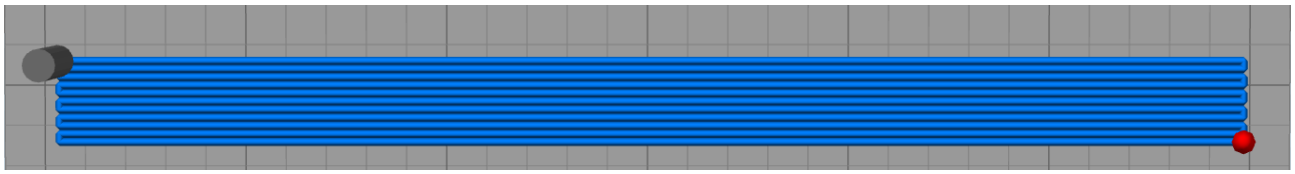

Fig. 18. Printing path of tensile specimen, view from top

2.6. Determination of the Void Content, Matrix and Fibre Volume in Composites

Void content in a composite structure can be determined by using destructive or non-destructive test methods [73]. A destructive test method can be accomplished by applying the ASTM D3171 standard [74]. This method provides better results than non-destructive, but the test specimens can no longer be used for other tests. Therefore, to avoid this, a non-destructive method can be used, such as the one specified in the ASTM D2734 standard [75]. The amount of air voids in the composite structure defines the mechanical properties of the composite. A lower air void content results in better mechanical properties. The amount of fibre and matrix in the composite also has a significant impact. A higher fibre content in the composite structure usually results in better mechanical properties.

To determine the matrix and fibre content in the composite structure and the void content, a non-destructive test method is chosen. The printed specimens were weighed and measured, and calculations were performed in accordance with ASTM D2734. Before measuring and weighing, the tensile and flexural specimens were prepared by trimming their ends in order to obtain more accurate results (Fig. 19.).

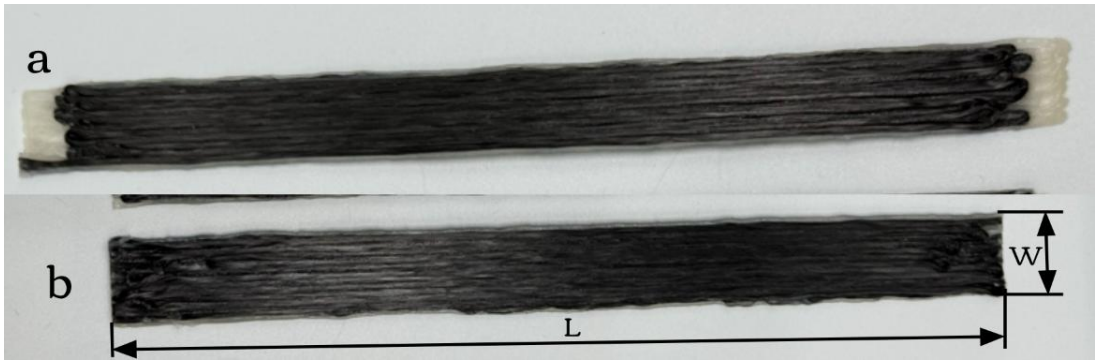

Fig. 19. Composite specimen: a – printed specimen without post-processing, b – specimen with trimmed ends (L – specimen length, W – specimen width)

The processed specimens were weighed using "BLOW JS13" scales with ±0.01 g measurement accuracy. Specimens length (L), width (W) and height (H), measured using a digital calliper. First, the amount of fibre content in the composite is calculated using this equation:

$$r = \frac{UL*L*MUL}{m} * 100 \quad (5)$$

where r – reinforcement in composite, weight %; UL – unidirectional lines of fibres; L – specimens length, mm; MUL – mass per unit length of used fibre, g/mm; m – specimens mass, g. Unidirectional line number depended on specimen type: the tensile specimen had 22 unidirectional lines, and the

flexural specimen had 72. Mass per unit length of the used pure fibre is taken from RC calculations. Later matrix content in the composite structure is calculated using the following equation:

$$R = 100 - r \tag{6}$$

where R – resin in composite, weight %; r – reinforcement in composite, weight %. Eventually, the void air content in the composite specimen is determined by using the following equation:

$$V = 100 - M_d\left(\frac{R}{D} + \frac{r}{d}\right) \tag{7}$$

where V – void content, volume %; M_d – measured composite density, g/cm^3; R – resin in composite, weight %; D – density of resin, g/cm^3; r – reinforcement in composite, weight %; R – density of reinforcing fibre, g/cm^3. PHA and PHBH/PBS blend biopolymers have a 1.24 g/cm^3 density. This value is used as the density of resin. The density value of the reinforcing fibre is chosen based on the synthetic fibre used in a composite. For carbon fibre 1.8 g/cm^3, for glass fibre 2.55 g/cm^3 and for aramid fibre 1.44 g/cm^3, density values were used. The density of the composites was calculated based on the specimens dimensions and weight using the following equation:

$$M_d = \frac{m}{L*W*H} \tag{8}$$

where M_d – measured composite density, g/cm^3; m – specimens mass, g; L – specimens length, cm; W – specimens width, cm; H – specimens height, cm.

2.7. Mechanical Testing on Composites

A universal testing machine, “Tinius Olsen M25KT”, is used to determine the mechanical properties of the printed composite structures. Tensile and flexural tests were conducted in accordance with ASTM D3039 and ASTM D7264. In total, 12 groups of 5 specimens for each group were prepared for these tests. 30 specimens were prepared for tensile tests, and another 30 specimens were prepared for flexural tests. The groups were classified according to the matrix material and reinforcing synthetic fibres used in composite structures. All fibres used in the composites were impregnated with PHBH/PBS blend biopolymer.

2.7.1. Tensile Testing

Tensile test specimens were prepared, and the tests were conducted in accordance with ASTM D3039. Before tensile testing, the printed specimens were prepared by cutting off the ends, weighing and measuring all dimensions, such as length, width and height, then affixing tabs, produced from PLA with 40x13x2 mm dimensions and 20° angle. Tabs were designed and attached to reduce stress concentrations. Also, points were marked that would allow to determine longitudinal and transverse deformations during the testing (Fig. 20.).

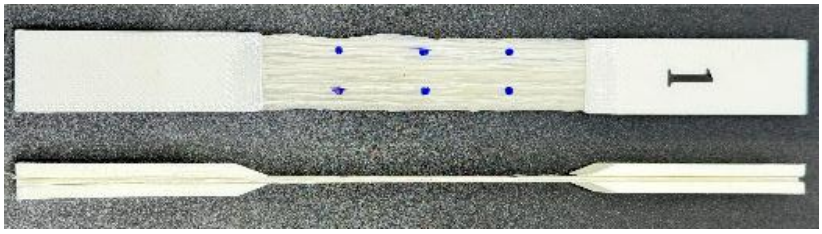

Fig. 20. Prepared tensile specimen, view from top and side

A “Tinius Olsen VEM 300” video extensometer with a “Still Optics” lens is used to measure the deformations. Before performing the tests, measurement points were selected in the software (Fig. 21.).

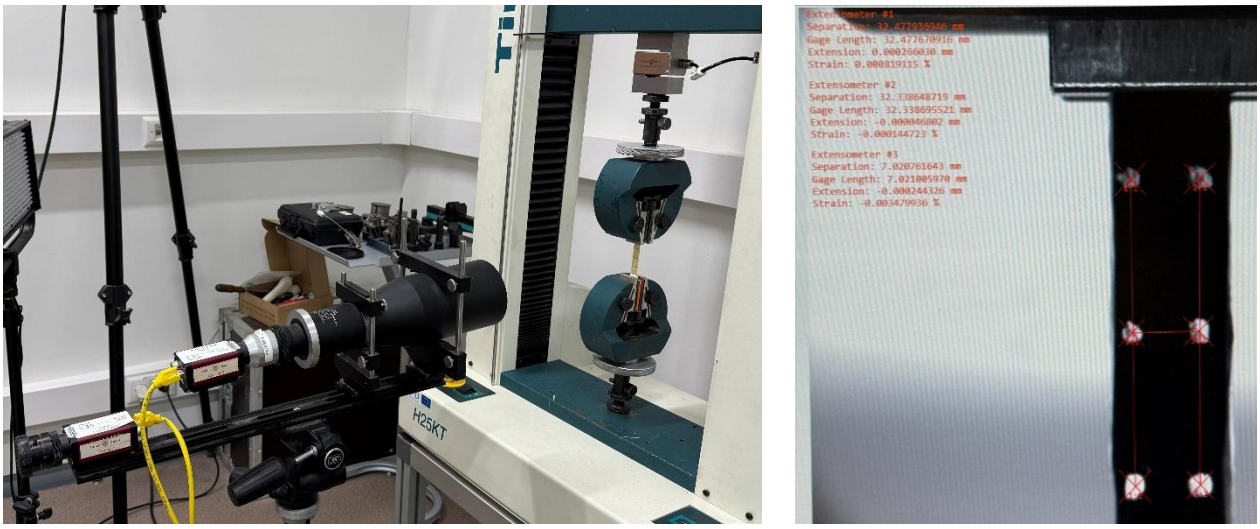

a b

Fig. 21. Tensile testing setup: a – video extensometer and testing machine, b – selected points in software

The tensile tests is performed by placing the specimen in the machine grips (Fig. 22.). To ensure that the specimens were positioned identically, a positioning plate is used, which is placed in the lower grip. A loading rate of 2 mm/min is selected for the tests.

Fig. 22. Tensile specimen placed in the grips

During the test, the specimen is pulled until it breaks. Only the force data is obtained, while strains are determined by a video extensometer. Therefore, to determine the mechanical properties of the composite structure, it is necessary to calculate the tensile strength (σ) and the Young’s modulus (E). The tensile strength is calculated using the following equation:

$$\sigma = \frac{F}{A} \tag{9}$$

where σ – ultimate tensile strength, MPa; F – maximum load before failure, N; A – average cross-sectional area, mm^2. The Young’s modulus is calculated using the following equation:

$$E = \frac{\Delta\sigma}{\Delta\varepsilon} \quad (10)$$

where E – Young's modulus, MPa; $\Delta\sigma$ – difference between the tensile stresses applied between two points of deformation, MPa; $\Delta\varepsilon$ – difference between two points of deformation, 0.003-0.002 (nominally 0.0025).

2.7.2. Flexural Testing

The flexural test is performed in accordance with ASTM D7264. The specimens were only prepared by cutting off the ends, weighing and measuring length, width and height. A 3-point bending test method is used (Fig. 23.), in which a specimen is placed on two support rollers with a distance of 80 mm, which is selected by the span-to-thickness ratio of 20:1. The span-to-thickness ratio is chosen so that the specimens length would be about 20% longer than the support span. The support span is chosen by the average flexural specimen thickness, which was 4 mm. The selected testing speed is 2 mm/min of crosshead movement.

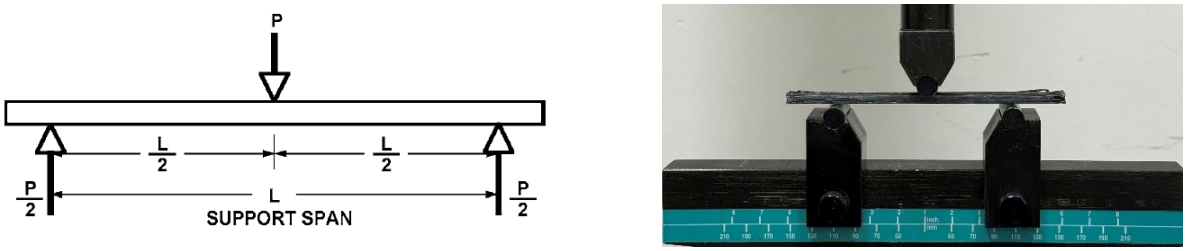

a b

Fig. 23. 3-point bending test: a – loading diagram [68], b – during bending testing

During testing, displacement and force acting on the specimen are obtained. Therefore, flexural strength is calculated using the following equation:

$$\sigma = \frac{3PL}{2bh^2} \quad (11)$$

where σ – flexural strength, MPa; P – maximum force acting on specimen, N; L – distance between the support rollers, mm; b – width of the specimen, mm; h – height of the specimen, mm. To calculate the flexural modulus, firstly, the maximum strain at the outer surface has to be calculated using the following equation:

$$\varepsilon = \frac{6\delta h}{L^2} \quad (12)$$

where ε – maximum strain at the outer surface, mm/mm; δ – mid-span deflection, mm; h – height of the specimen, mm; L – support span, mm. The flexural modulus is calculated using the following equation:

$$E = \frac{\Delta\sigma}{\Delta\varepsilon} \quad (13)$$

where E – flexural modulus, MPa; $\Delta\sigma$ – difference between the flexural stresses applied between two points of deformation, MPa; $\Delta\varepsilon$ – difference between two points of deformation, 0.003-0.002 (nominally 0.0025).

2.8. Chapter Summary

The objective of this study is to investigate the mechanical properties of composite structures composed of biopolymers and synthetic fibres manufactured using AM technology. This chapter describes the biopolymer matrix and synthetic reinforcement materials used for the production of composite structures. The section describes the preparation of synthetic towpregs for additive manufacturing using the melt impregnation method, where continuous synthetic fibres are embedded with PHBH/PBS blend biopolymer matrix. The quality of the fibre impregnation is determined by the amount of resin absorbed by the fibre, which is calculated in accordance with the ASTM D4018 standard. The chapter covers the pull-out test method procedure, which is used to determine the interfacial shear strength of synthetic fibres and biopolymers, as well as the effect of impregnation on IFSS. This section also describes how AM technologies were used to produce composite specimens for tensile and flexural tests. Presented as the fibre, matrix, and air void content in a composite structure, determined in accordance with ASTM D2734. It is also presented how, in accordance with ASTM D3039 and ASTM D7264 standards, tensile and flexural tests were performed to determine the mechanical properties of composite structures composed of biopolymers and synthetic fibres manufactured using AM technology.

3. Resin Content Evaluation, Interfacial Shear Strength Determination, Tensile and Flexural Test Results of Composite Structures

3.1. Resin Content of Impregnated Synthetic Fibres

Continuous carbon fibre towpregs (Fig. 24.) were prepared for additive manufacturing by melt impregnating 3K carbon fibre with PHBH/PBS blend polymer. After impregnating the fibre, it was observed that the polymer was not distributed evenly along the entire length of the fibre, but the entire surface of the fibre was coated with polymer matrix, which made the fibre suitable for use in additive manufacturing of composite materials and less prone to damage.

Fig. 24. 3K carbon fibre towpreg

To evaluate the quality of 3K carbon fibre impregnation, resin content calculations were performed, the results of which are presented in Table 5. The samples were randomly selected from different sections of the continuous impregnated carbon fibre tow.

Table 5. Resin content of prepared 3K carbon fibre towpreg

Sample No.	Pure 3K CF, mg/m	Impregnated 3K CF, mg/m	RC, %	Fibre content, %
1	201.3	309.6	34.98%	65.02%
2	201	245.3	18.06%	81.94%
3	201.9	309.8	34.83%	65.17%
4	203.4	339.3	40.05%	59.95%
5	205.3	252.7	18.76%	81.24%
6	202.2	246.1	17.84%	82.16%
7	200.2	254.1	21.21%	78.79%
8	201.3	259.2	22.34%	77.66%
9	204.5	243.8	16.12%	83.88%
10	203.4	259.6	21.65%	78.35%
Average	**202.45±1.6**	**271.95±34.3**	**24.58±8.63%**	**75.42%±8.63%**

The results presented show that the mass per unit length of pure 3K CF, on average, is 0.202 g/m, and the impregnated fibres are 0.272 g/m. This means that this towpreg on average contains 24.58% of resin by weight. Resin content of CF towpreg ranged from 16.12% to 40.05%, and the results had

8.63% standard deviation. Such a large, uneven matrix distribution over the fibre can lead to the formation of larger voids in composite structures and poorer dimensional accuracy in printed parts.

Continuous glass fibre towpregs (Fig. 25.) were prepared similarly to 3K CF towpreg. After impregnation, it was observed that glass fibre absorbs PHBH/PBS polymer similarly to carbon fibre. However, the impregnation process for glass fibre is simpler because it is more resistant to breakage than carbon fibre.

Fig. 25. Glass fibre towpreg

To evaluate the quality of glass fibre impregnation, resin content calculations were performed, the results of which are presented in Table 6. The samples were randomly selected from different sections of the continuous impregnated glass fibre tow. In a similar way as it was done with carbon fibre tow.

Table 6. Resin content of prepared glass fibre towpreg

Sample No.	**Pure GF, mg/m**	**Impregnated GF, mg/m**	**RC, %**	**Fibre content, %**
1	311.8	381.7	18.31%	81.69%
2	311.9	373.1	16.40%	83.60%
3	312.2	381.4	18.14%	81.86%
4	310.3	375.8	17.43%	82.57%
5	310	369.9	16.19%	83.81%
6	312.8	340	8.00%	92.00%
7	311.4	367.2	15.20%	84.80%
8	311.5	343.2	9.24%	90.76%
9	309.8	374.8	17.34%	82.66%
10	310.2	361.5	14.19%	85.81%
Average	**311.19±1.0**	**366.86±14.7**	**15.04±3.63%**	**84.96±3.63%**

The results presented show that the mass per unit length of pure glass fibre, on average, is 0.311 g/m, and the impregnated glass fibres are 0.367 g/m. This means that glass fibre towpreg on average contains 15.04% of resin by weight. Resin content of CF towpreg ranged from 9.24% to 18.31%, and the results had 3.64% standard deviation. These results show that the glass fibre impregnated with PHBH/PBS is impregnated more uniformly, but a smaller amount of the matrix agent covers the fibre

itself compared to carbon fibre towpreg. To produce glass fibre towpregs with higher matrix content, different impregnation process parameters and a larger outlet nozzle should be used.

Continuous aramid fibre towpreg (Fig. 26.) prepared in the same way as other synthetic fibre towpregs. This aramid towpreg, even after being impregnated with a biopolymer matrix, remained just as flexible as the unimpregnated fibre and had randomly formed lumps. Towpregs flexibility did not cause any problems during composite printing, but lumps could have caused issues during printing, so towpreg was passed through the heating block again to remove the lumps.

Fig. 26. Aramid fibre towpreg

To evaluate the quality of aramid fibre impregnation, resin content calculations were performed, the results of which are presented in Table 7. The samples were randomly selected from different sections of the continuous impregnated aramid fibre tow. In a similar way to how it was done with other synthetic fibre tows.

Table 7. Resin content of prepared aramid fibre towpreg

Sample No.	**Pure AF, mg/m**	**Impregnated AF, mg/m**	**RC, %**	**Fibre content, %**
1	86.4	154.7	44.15%	55.85%
2	86	162.9	47.21%	52.79%
3	85.6	116.1	26.27%	73.73%
4	85.3	116.9	27.03%	72.97%
5	85.1	101.5	16.16%	83.84%
6	86.1	122.5	29.71%	70.29%
7	86.2	116.3	25.88%	74.12%
8	85.4	147.8	42.22%	57.78%
9	85.1	127.4	33.20%	66.80%
10	85.3	176.4	51.64%	48.36%
Average	**85.65±0.5**	**134.25±24.5**	**34.35±11.39%**	**65.65±11.39%**

The results presented show that the mass per unit length of pure aramid fibre, on average, is 0.086 g/m, and the impregnated aramid fibres are 0.134 g/m. This means that aramid fibre towpreg, on average, contains 34.35% of resin by weight. Resin content of AF towpreg ranged from 16.16% to 51.64%, and the results had 11.39% standard deviation. Aramid fibre towpreg had the highest resin content, but it also had the most uneven distribution of the matrix material, compared to other synthetic fibres.

3.2. Interfacial Shear Strength Test Results

Initial test of interfacial shear strength test to determine the compatibility of the synthetic fibres and biopolymers was performed with PHA and unimpregnated fibres (Fig. 27.).

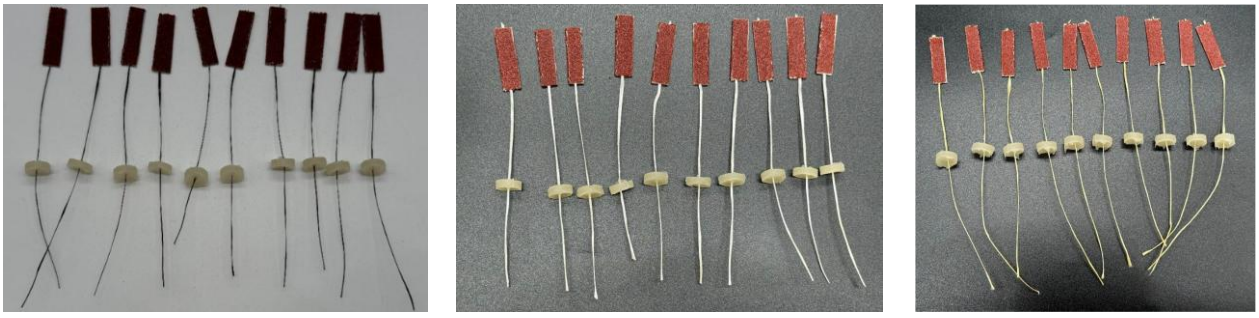

a b c

Fig. 27. IFSS specimens with unimpregnated synthetic fibres and 0.25 g of PHA matrix: a – PHA/CFn, b – PHA/GFn, c – PHA/AFn

Results of adhesion tests of PHA and unimpregnated synthetic fibres are presented in Table 8. To obtain more accurate results, some data values were removed from the calculation.

Table 8. Pull-out test results of specimens with PHA and unimpregnated synthetic fibres

Specimen type	Maximum force, N	Embedded fibres length, mm	IFSS, MPa
PHA/CFn	70.83±6.82	3.78±0.64	**17.6±4.4**
PHA/GFn	50.56±8.91	3.99±0.28	**10.4±1.7**
PHA/AFn	27.92±4.5	3.8±0.21	**6.1±1.2**

The results show that carbon fibre had the highest IFSS with PHA, and it is the most compatible one with this biopolymer, compared to other synthetic fibres. 3K CF interfacial strength with PHA polymer was 17.6 MPa on average. While other fibres such as GF, have only 10.4 MPa of IFSS on average, and AF only have 6.1 MPa of IFSS on average, with PHA. Similar IFSS specimens with PHBH/PBS blend matrix and unimpregnated synthetic fibres (Fig. 28.) were prepared, and the same pull-out tests were performed to determine whether synthetic fibres are more compatible with PHA or PHBH/PBS biopolymers.

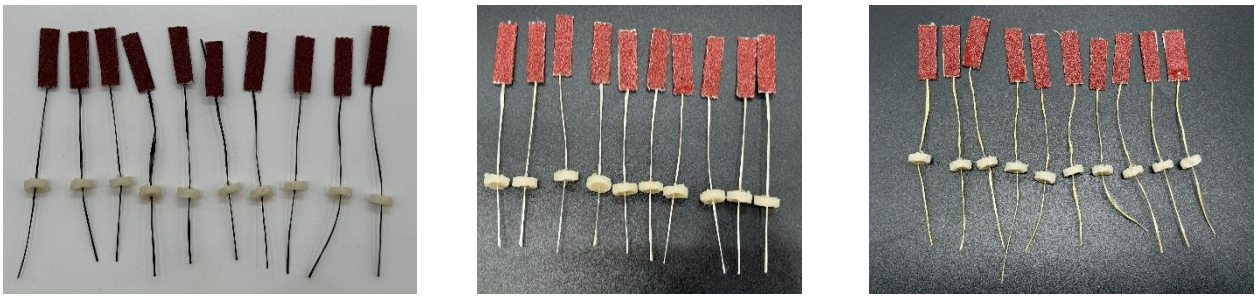

a b c

Fig. 28. IFSS specimens with unimpregnated synthetic fibres and 0.3 g of PHBH/PBS blend matrix: a – (PHBH/PBS)/CFn, b – (PHBH/PBS)/GFn, c – (PHBH/PBS)/AFn

Results of adhesion tests of PHBH/PBS matrix and unimpregnated synthetic fibres are presented in Table 9. During testing, not all of the fibres pulled out of the matrix plate. Some of the specimens broke, and those values of broken synthetic fibres were not included in the calculations.

Table 9. Pull-out test results of specimens with PHBH/PBS and unimpregnated synthetic fibres

Specimen type	Maximum force, N	Embedded fibres length, mm	IFSS, MPa
(PHBH/PBS)/CFn	115±8.49	4.14±0.35	**22.8±2.6**
(PHBH/PBS)/GFn	60.13±2.86	4.21±0.22	**11.68±0.29**
(PHBH/PBS)/AFn	49.31±5.76	4.34±0.25	**12.93±1.45**

The results show that synthetic fibres are more compatible with PHBH/PBS blend polymer than with PHA. CF had 29.5% higher IFSS with PHBH/PBS blend than with PHA matrix. Glass fibre only had 12.3% higher IFSS on average than with PHA, and aramid fibre had 2 times higher IFSS with PHBH/PBS than with PHA. Also, it was noted that AF is more compatible with PHBH/PBS than GF. To determine the effect of impregnation on the adhesion strength between synthetic fibres and biopolymers, pull-out tests were performed on IFSS specimens with melt impregnated synthetic fibres and PHA matrix (Fig. 29.). Experiments with this type of specimens also helped to determine the function of PHBH/PBS as an interface between synthetic fibres and the PHA matrix.

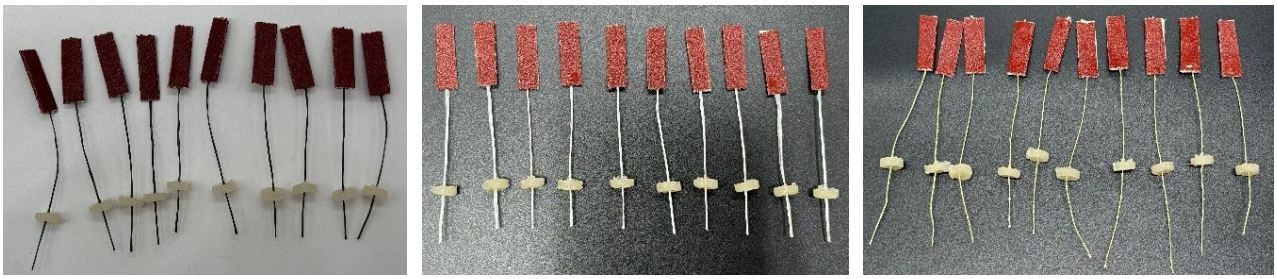

a b c

Fig. 29. IFSS specimens with melt impregnated synthetic fibres and 0.3 g of PHA matrix: a – PHA/CFm, b – PHA/GFm, c – PHA/AFm

Results of adhesion tests of PHA matrix and synthetic towpregs are presented in Table 10.

Table 10. Pull-out test results of specimens with PHA and synthetic fibre towpregs

Specimen type	Maximum force, N	Embedded fibres length, mm	IFSS, MPa
PHA/CFm	93.67±25.09	3.96±0.34	**19.66±5.96**
PHA/GFm	105.23±6.71	4.36±0.26	**19.72±0.93**
PHA/AFm	52.5±5.14	4.57±0.39	**13.13±1.6**

The results show that GF towpreg had the highest IFSS strength with PHA polymer, than other synthetic towpregs. Overall, it had similar IFSS strength as CF towpreg. Results also show that impregnation helped to improve IFSS between the PHA biopolymer and synthetic fibres. By impregnating CF with PHBH/PBS, IFSS was improved by 11.7%, GF IFSS was improved by 89.6%, and AF IFSS with PHA was improved by 115.2%. These results also indicate that PHBH/PBS is suitable as an interface material between the PHA matrix and reinforcing synthetic fibres. Similar

IFSS specimens with PHBH/PBS blend matrix and synthetic towpregs (Fig. 30.) were prepared, and the same pull-out tests were performed.

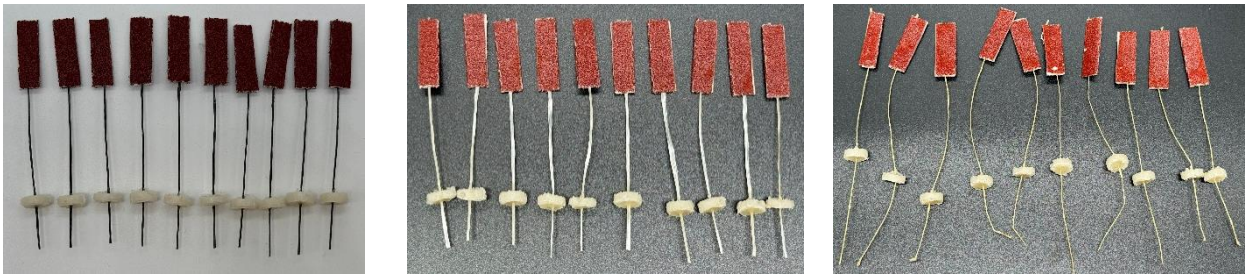

a b c

Fig. 30. IFSS specimens with melt impregnated synthetic fibres and 0.3 g of PHBH/PBS blend matrix: a – (PHBH/PBS)/CFm, b – (PHBH/PBS)/GFm, c – (PHBH/PBS)/AFm

Results of adhesion tests of PHBH/PBS matrix and synthetic towpregs are presented in Table 11.

Table 11. Pull-out test results of specimens with PHBH/PBS and synthetic fibre towpregs

Specimen type	Maximum force, N	Embedded fibres length, mm	IFSS, MPa
(PHBH/PBS)/CFm	142.47±7.64	4.29±0.27	**27.21±2.27**
(PHBH/PBS)/GFm	108.52±16.65	4.36±0.24	**20.42±3.66**
(PHBH/PBS)/AFm	43.54±3.21	5.25±0.22	**9.46±0.90**

The results show that CF towpreg had the highest IFSS with PHBH/PBS matrix. By impregnating carbon fibre with PHBH/PBS, IFSS was improved by 19.3 %, and GF IFSS with this matrix was improved by 74.8%. Similar improvements were made with the PHA matrix. Therefore, these results show that by impregnating carbon and glass fibres with PHBH/PBS blend polymer, their interfacial strength with the matrix material can be improved. However, after impregnating the aramid fibre, its IFSS with PHBH/PBS decreased by 26.8%. This result shows that impregnation does not always improve material compatibility. Furthermore, this result indicates that the PHBH/PBS composite reinforced with AF would have poorer mechanical properties than the PHA/AF composite structure.

3.3. Results of Tensile Tests

3.3.1. Tensile Test Results of Composites Composed of PHA and Synthetic Fibres

A total of 15 composite specimens were printed with a PHA matrix (Fig. 31.): 5 specimens were reinforced with continuous carbon fibre towpreg (PHA/CF), 5 with continuous glass fibre towpreg (PHA/GF), and 5 with continuous aramid fibre towpreg (PHA/AF). All synthetic towpregs were impregnated with PHBH/PBS blend biopolymer. Thermally processed PHA stays soft and elastic longer than other thermoplastics. Therefore, after printing the composite specimen, it was left on the build plate to cool off at room temperature for at least 30 minutes to ensure that the shape and dimensions of the specimen remain unaffected. After being removed from the printing platform, samples were weighed, measured and mechanical tests performed at least one day after their production. It was also observed that during printing, due to the longer crystallization time of this matrix material, it is more difficult to produce precise composites. This means that every time the printing trajectory changes, the synthetic fibre is being dragged across the printed composites top

surface because the matrix material, which has not yet fully cured, does not hold the deposited towpreg in place.

a b c

Fig. 31. Printed composite tensile specimens: a – PHA/CF, b – PHA/GF, c – PHA/AF

The printed tensile specimens with PHA matrix after processing were weighed and measured. The weights, dimensions and calculated composite fibre, matrix and void contents are presented in Table 12.

Table 12. Dimensions, weights, and fibre, matrix, and void contents of a composite tensile specimen with a PHA matrix

Specimen type	**S. No**	**Length, mm**	**Width, mm**	**Height, mm**	**Cross-sectional area, mm2**	**Weight, g**	**Fibre content, weight %**	**Matrix content, weight %**	**Void content, volume %**
PHA/CF	1.	126.54	12.87	1.01	13.00	1.78	31.7%	68.3%	21.3%
	2.	127.53	12.86	1.01	12.99	1.71	33.2%	66.8%	25.4%
	3.	127.91	12.96	0.98	12.70	1.77	32.2%	67.8%	20.9%
	4.	127.80	12.93	1.01	13.06	1.77	32.2%	67.8%	23.0%
	5.	126.79	13.07	1.04	13.59	1.80	31.4%	68.6%	24.0%
	Average	**127.31**	**12.94**	**1.01**	**13.07**	**1.77**	**32.1%**	**67.9%**	**22.9%**
PHA/GF	1.	128.19	12.79	1.02	13.05	1.99	44.1%	55.9%	25.8%
	2.	127.66	12.62	1.01	12.75	1.99	43.9%	56.1%	23.6%
	3.	126.92	12.54	1.00	12.54	1.93	45.0%	55.0%	24.8%
	4.	128.19	12.61	0.98	12.36	2.00	43.9%	56.1%	21.1%
	5.	129.07	12.48	1.01	12.60	1.94	45.5%	54.5%	26.3%
	Average	**128.01**	**12.61**	**1.00**	**12.66**	**1.97**	**44.5%**	**55.5%**	**24.3%**
PHA/AF	1.	126.44	11.49	0.99	11.38	1.36	17.5%	82.5%	25.6%
	2.	126.61	11.47	0.99	11.36	1.37	17.4%	82.6%	25.0%
	3.	127.17	11.66	1.00	11.66	1.41	17.0%	83.0%	25.1%
	4.	126.42	11.83	0.99	11.71	1.42	16.8%	83.2%	24.5%
	5.	127.32	11.82	1.00	11.82	1.42	16.9%	83.1%	25.7%
	Average	**126.79**	**11.65**	**0.99**	**11.58**	**1.40**	**17.1%**	**82.9%**	**25.2%**

The results show that the printed specimens had quite consistent dimensions. The most consistent measurement was the height, which remained consistent over different types of composites. The composites reinforced with GF and CF exhibited a larger width than the composites reinforced with AF. Although the same parameters were used to manufacture all these specimens, this may have been due to the smaller fibre tow size. The analytically calculated density of these composites is 1.06 g/cm^3 of PHA/CF, 1.22 g/cm^3 of PHA/GF, and 0.95 g/cm^3 of PHA/AF on average. Overall, the PHA/GF composite had the highest analytical density, weight, and fibre content among other types of composites. The total void content volume of all composite types varies between 22.9% and 25.2%. These values are quite high, but it is unlikely to have a significant impact on the tensile strength. The amount of fibre may have a greater impact on these strengths. After measuring the printed composites, the specimens with PHA matrix were prepared for tensile testing (Fig. 32.), the tabs were attached, and deformation points marked.

a b c

Fig. 32. Prepared composite tensile specimens: a – PHA/CF, b – PHA/GF, c – PHA/AF

The forces obtained during the tensile testing on composite tensile specimens with PHA matrix and the calculated tensile strength, along with Young's modulus, are presented in Table 13.

Table 13. Mechanical properties of composite tensile specimens with PHA matrix

Composite type	**Specimen No.**	**Maximum force, N**	**Tensile strength, MPa**	**Young's modulus, GPa**
PHA/CF	1.	3551	294.7	41.71
	2.	4258	337.5	34.27
	3.	4181	350.0	36.57
	4.	4775	389.5	35.35
	5.	3213	272.0	41.96
	Average	**3996±617**	**328.7±46.4**	**37.97±3.62**
PHA/GF	1.	4680	388.4	16.28
	2.	4395	348.4	15.13
	3.	4838	405.0	14.95
	4.	5057	412.5	16.03
	5.	4585	388.1	15.77
	Average	**4711±251**	**388.5±24.8**	**15.63±0.58**

Composite type	Specimen No.	Maximum force, N	Tensile strength, MPa	Young's modulus, GPa
PHA/AF	1.	2697	223.8	10.34
	2.	2618	207.5	9.81
	3.	2565	214.7	9.11
	4.	2718	221.7	9.54
	5.	2548	215.7	10.43
	Average	**2629±76**	**216.7±6.4**	**9.84±0.55**

The results show that composite specimens, where PHA is reinforced with GF, had a higher tensile strength than those reinforced with other synthetic fibres. PHA/GF had the 388.5 MPa tensile strength, which is 18.2% higher than PHA/CF composites and 79.3% higher than PHA/AF composites tensile strengths, on average. Also, the PHA/CF composite type had the highest Young's modulus, meaning it was stiffer than other composite structures. The PHA/CF composite structure type had 142.9% higher Young's modulus than the PHA/GF, and 285.87% higher than the PHA/AF composite type. Overall, all these composite materials exhibited excellent mechanical properties, which had higher tensile strengths and Young's modulus than high-performance engineering thermoplastics such as polyetheretherketone (PEEK). The PHA/CF composite after tensile testing and stress-strain curves are shown in Figure 33.

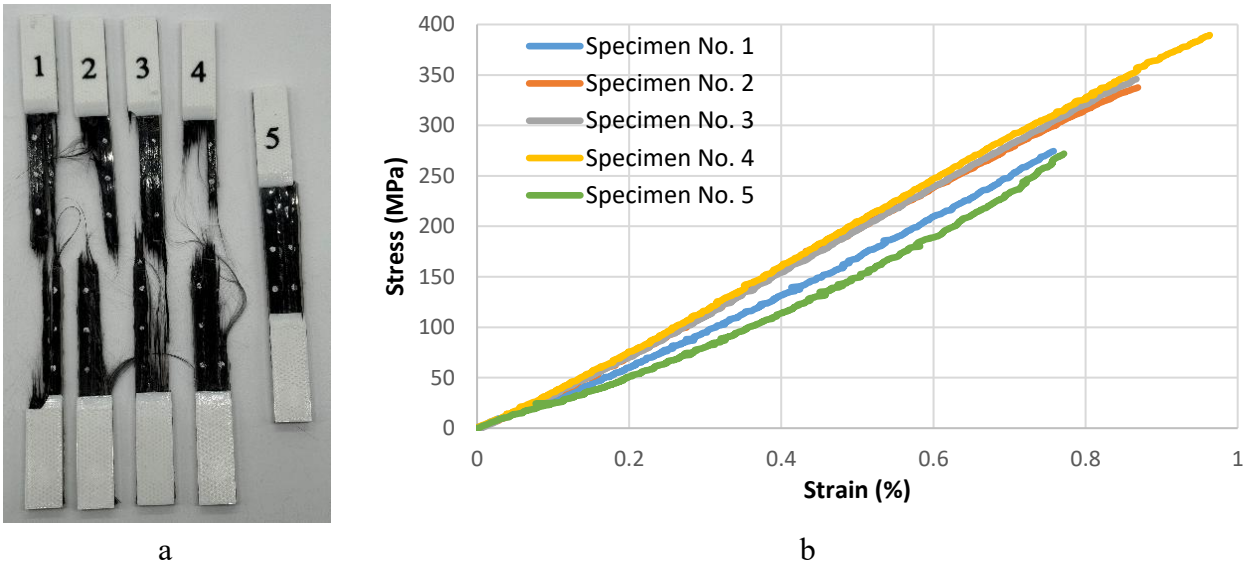

a b

Fig. 33. PHA/CF composite results after tensile testing: a – broken composites, b – stress-strain curves

The tensile strength results of PHA/CF composites ranged from 271.95 to 389.48 MPa. Standard deviation and variation coefficient were 46.4 and 14.1%, respectively. Therefore, these results can be considered not as reliable as other specimen type results. Such a large distribution of results could have caused damaged fibres during the impregnation and printing process, and unevenly impregnated fibres. From stress-strain curves, it can be seen that PHA/CF composites strain at break ranged from 0.8% to 1%. Moreover, these samples mostly exhibited SGM failure mode, which is determined in accordance with the ASTM D3039 standard. The specimen No. 5 had the lowest tensile strength, and it is the only specimen that was not separated into two pieces after breaking. The PHA/GF composite after tensile testing and stress-strain curves are shown in Figure 34.

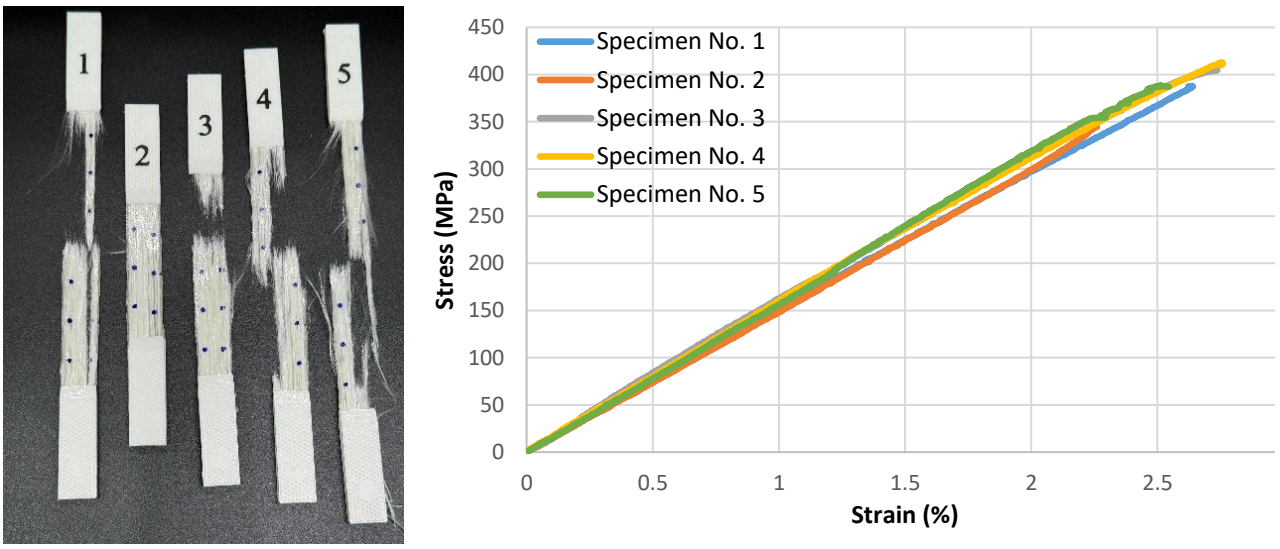

a b

Fig. 34. PHA/GF composite results after tensile testing: a – broken composites, b – stress-strain curves

Although the stress-strain curves of the PHA/GF composites are similar, the tensile strength results ranged from 348.4 to 412.5 MPa. Standard deviation and variation coefficient of tensile test results were 24.8 and 6.4%, respectively. The distribution of test results shows that the glass fibres were not as severely damaged as the carbon fibres, during the production process. Moreover, PHA/GF composite specimens mostly exhibited SGM failure modes, and specimen No. 3 had a LAT failure mode. Also, during tensile testing, glass fibres inside the specimens started breaking sequentially before fully breaking. The PHA/AF composite after tensile testing and stress-strain curves are shown in Figure 35.

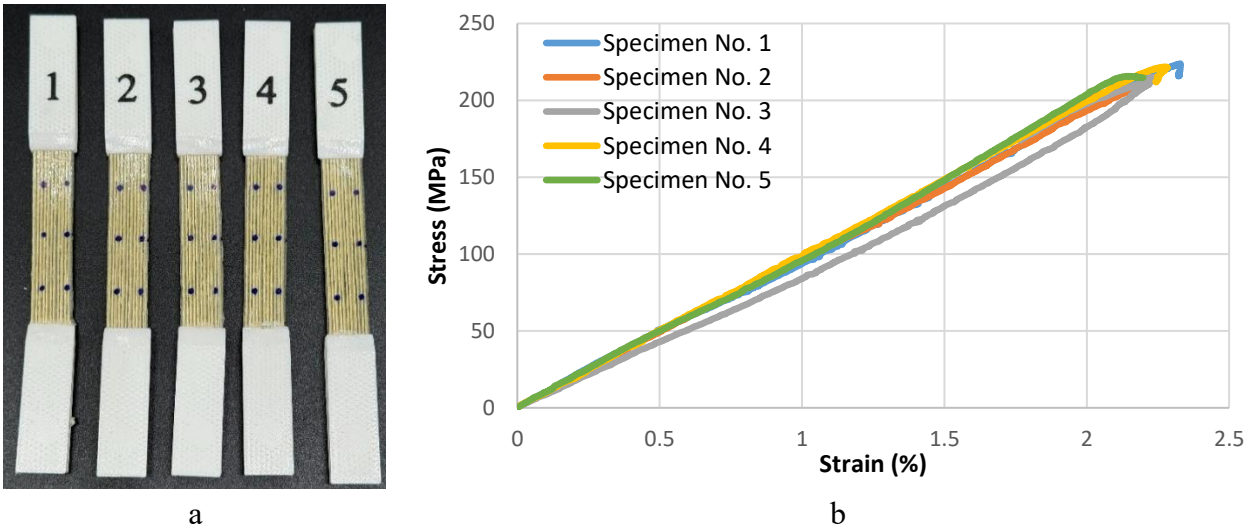

a b

Fig. 35. PHA/AF composite results after tensile testing: a – broken composites, b – stress-strain curves

The tensile strength results of PHA/AF composites ranged from 207.53 to 223.85 MPa. Standard deviation and variation coefficient were 6.4 and 3%, respectively. These samples exhibited LIT and SIM failure modes. Also, composites reinforced with continuous aramid fibres after the tensile test did not break into two separate pieces. Overall, all PHA/AF composite tensile specimens exhibited similar results. However, these composite structures had the lowest tensile strength and Young's modulus compared to composites reinforced with carbon or glass fibres.

3.3.2. Tensile Test Results of Composites Composed of PHBH/PBS and Synthetic Fibres

A total of 15 composite specimens were printed with a PHBH/PBS matrix (Fig. 36.): 5 specimens were reinforced with continuous carbon fibre towpreg ((PHBH/PBS)/CF), 5 with continuous glass fibre towpreg ((PHBH/PBS)/GF), and 5 with continuous aramid fibre towpreg ((PHBH/PBS)/AF).

a b c

Fig. 36. Printed composite tensile specimens: a – (PHBH/PBS)/CF, b – (PHBH/PBS)//GF, c – (PHBH/PBS)//AF

The printing process was significantly simpler and easier when using a PHBH/PBS matrix compared to PHA. Once printing was complete, there was no need to wait that long before removing the printed composite structure from the build platform. These specimens are also distinguished by their smoother edges and smoother surface. The printed tensile specimens with the PHBH/PBS matrix after processing were weighed and measured. The weights, dimensions and calculated composite fibre, matrix and void contents are presented in Table 14.

Table 14. Dimensions, weights, and fibre, matrix, and void contents of a composite tensile specimen with a PHBH/PBS matrix

Specimen type	S. No	Length, mm	Width, mm	Height, mm	Cross-sectional area, mm2	Weight, g	Fibre content, weight %	Matrix content, weight %	Void content, volume %
(PHBH/PBS)/CF	1.	133.13	11.85	1.25	14.81	1.87	31.7%	68.3%	31.1%
	2.	132.79	12.63	1.09	13.77	1.73	34.2%	65.8%	31.8%
	3.	134.20	13.02	1.06	13.80	1.77	33.8%	66.2%	31.0%
	4.	132.92	12.49	1.16	14.49	1.78	33.3%	66.7%	33.2%
	5.	134.64	12.57	1.13	14.20	1.80	33.3%	66.7%	32.0%
	Average	**133.54**	**12.51**	**1.14**	**14.21**	**1.79**	**33.3%**	**66.7%**	**31.8%**
(PHBH/PBS)/GF	1.	134.84	12.17	0.99	12.05	1.96	47.1%	52.9%	26.2%
	2.	134.17	12.49	1.01	12.61	2.1	43.7%	56.3%	22.4%
	3.	133.2	12.19	0.98	11.95	2.09	43.6%	56.4%	17.8%
	4.	135.04	12.26	1	12.26	2.04	45.3%	54.7%	23.8%
	5.	133.44	12.18	0.97	11.81	1.97	46.4%	53.6%	23.2%
	Average	**134.14**	**12.26**	**0.99**	**12.14**	**2.03**	**45.2%**	**54.8%**	**22.7%**

Specimen type	S. No	Length, mm	Width, mm	Height, mm	Cross-sectional area, mm2	Weight, g	Fibre content, weight %	Matrix content, weight %	Void content, volume %
(PHBH/PBS)/AF	1.	134.23	11.25	0.95	10.69	1.45	17.5%	82.5%	20.5%
	2.	134.71	11.31	0.95	10.74	1.44	17.6%	82.4%	21.7%
	3.	134.47	11.68	0.99	11.56	1.55	16.4%	83.6%	21.4%
	4.	134.82	11.57	0.98	11.34	1.49	17.1%	82.9%	23.3%
	5.	134.49	11.46	0.98	11.23	1.44	17.6%	82.4%	25.0%
	Average	**134.54**	**11.45**	**0.97**	**11.11**	**1.47**	**17.2%**	**82.8%**	**22.4%**

The results show that dimensions were quite similar to those of composites produced with a PHA matrix. Specimens had similar weights, fibre, matrix, and void contents. Overall, tensile specimens reinforced with CF had 32.7% of fibre content, with GF had 44.7%, and with AF 17.2%. The analytically calculated density of these composites is 0.94 g/cm3 of (PHBH/PBS)/CF, 1.25 g/cm3 of (PHBH/PBS)/GF, and 0.99 g/cm3 of (PHBH/PBS)/AF on average. (PHBH/PBS)/GF and (PHBH/PBS)/AF composites had similar and significantly lower void volume than (PHBH/PBS)/CF composites. Composites reinforced with aramid fibre had the lowest weight and the lowest amount of reinforcement in the structure, and composites reinforced with glass fibre had the highest weight and the highest amount of reinforcement in the structure. After measuring the printed composites, the specimens with PHBH/PBS matrix were prepared for tensile testing (Fig. 37.), the tabs were attached, and deformation points marked.

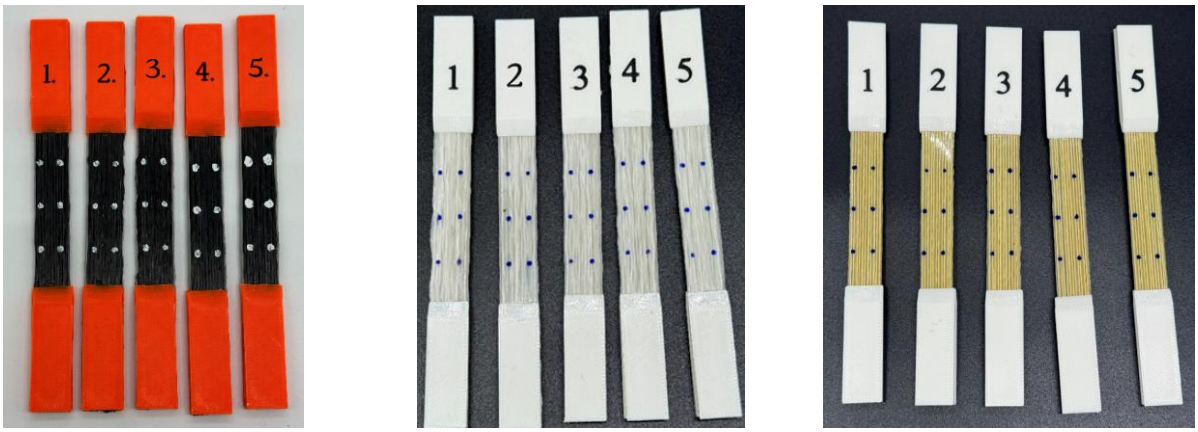

a b c

Fig. 37. Prepared composite tensile specimens: a – (PHBH/PBS)/CF, b – (PHBH/PBS)//GF, c – (PHBH/PBS)//AF

The forces obtained during the tensile testing on composite tensile specimens with PHBH/PBS matrix and the calculated tensile strength, along with Young's modulus, are presented in Table 15.

Table 15. Mechanical properties of composite tensile specimens with PHBH/PBS matrix

Composite type	Specimen No.	Maximum force, N	Tensile strength, MPa	Young's modulus, GPa
(PHBH/PBS)/CF	1.	3840	259.2	11.87
	2.	4511	327.7	26.86

Composite type	Specimen No.	Maximum force, N	Tensile strength, MPa	Young's modulus, GPa
	3.	4327	313.5	28.58
	4.	4199	289.8	28.58
	5.	4563	321.2	27.88
	Average	**4288±289**	**302.3±28.0**	**24.75±7.24**
(PHBH/PBS)/GF	1.	4716	391.4	14.19
	2.	4929	390.7	13.75
	3.	4673	391.2	14.18
	4.	4983	406.4	13.80
	5.	4682	396.3	14.70
	Average	**4798±148**	**395.2±6.7**	**14.12±0.38**
(PHBH/PBS)/AF	1.	3190	298.5	10.12
	2.	3223	300.0	9.94
	3.	2905	251.2	8.00
	4.	2771	244.4	8.25
	5.	3070	273.4	9.63
	Average	**3032±192**	**273.5±25.8**	**9.19±0.99**

The results show that (PHBH/PBS)/CF composites had moderate tensile strength, which was 302.3 MPa on average, and the highest Young's modulus, which was 24.75 GPa on average. This means that composite structures reinforced with carbon fibre are nearly twice as stiff as those reinforced with glass or aramid fibre. (PHBH/PBS)/GF type composite structure exhibited the highest tensile strength, which was 395.2 MPa, on average, and it was 30.7% higher than (PHBH/PBS)/CF composites, and 44.5% higher than (PHBH/PBS)/AF composites. These results were likely influenced by the fibre content in the composite. The (PHBH/PBS)/CF composite after tensile testing and stress-strain curves are shown in Figure 38.

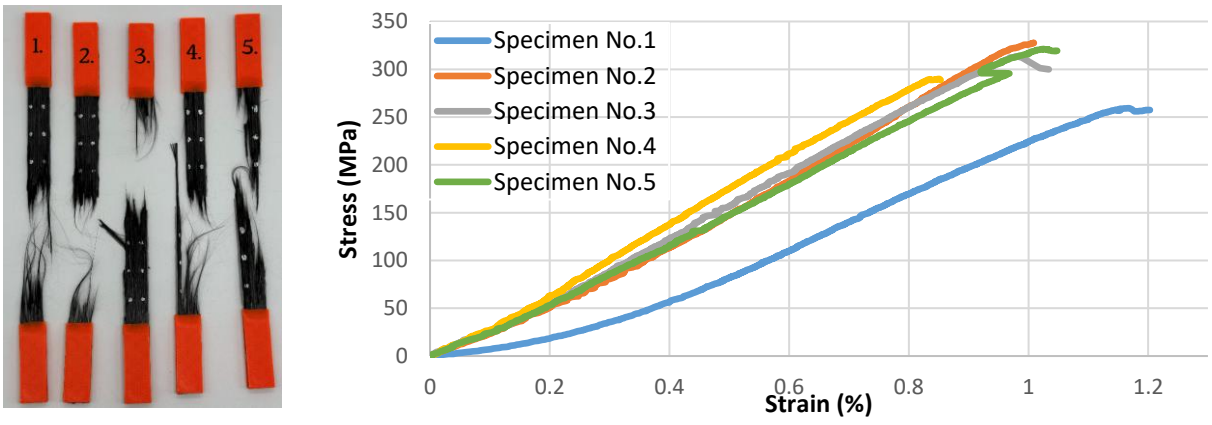

a b

Fig. 38. (PHBH/PBS)/CF composite results after tensile testing: a – broken composites, b – stress-strain curves

The tensile strength results of (PHBH/PBS)/CF composites ranged from 259.24 to 327.67 MPa. Standard deviation and variation coefficient were 28 and 9.3%, respectively. Therefore, these results

can be considered not as reliable as other specimen type results. Specimen No. 1 had the most influential impact on the distribution of the results. This specimen had 14.3% lower tensile strength and 52% lower Young's module than the averages of this type of composite. Moreover, these samples exhibited GAB, SGM, and SGR failure modes, which are determined in accordance with the ASTM D3039 standard. The first three exhibited a GAB failure mode, which means that these specimens had a grip failure type at the grip and at the bottom of the specimen. Other specimens had long splitting at the gage, and in the middle and one on the right. The (PHBH/PBS)/GF composite after tensile testing and stress-strain curves are shown in Figure 39.

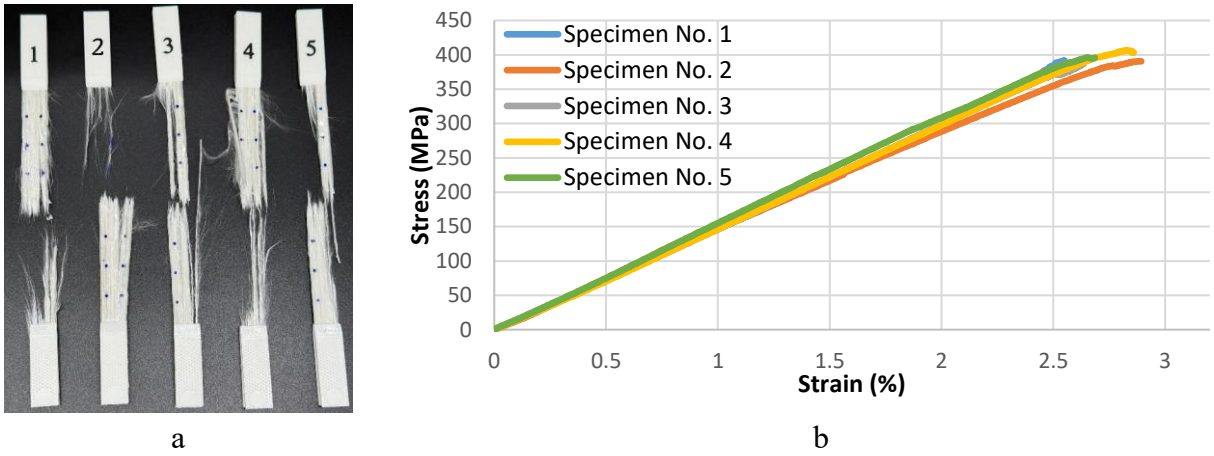

a b

Fig. 39. (PHBH/PBS)/GF composite results after tensile testing: a – broken composites, b – stress-strain curves

The results of (PHBH/PBS)/CF composites ranged from 390.73 to 406.44 MPa. Standard deviation and variation coefficient were 6.7 and 1.7%, respectively. Therefore, these results can be considered more reliable than those of (PHBH/PBS)/CF composites. Moreover, these samples exhibited XAB, XAT, and SGM failure modes. These are classified as explosive failure modes near the tab at the bottom or top of the specimen, and long gage splitting at the middle of the specimen. During tensile testing, before the composite specimen failed completely, the fibres broke one after another within the composite structure. The (PHBH/PBS)/AF composite after tensile testing and stress-strain curves are shown in Figure 40.

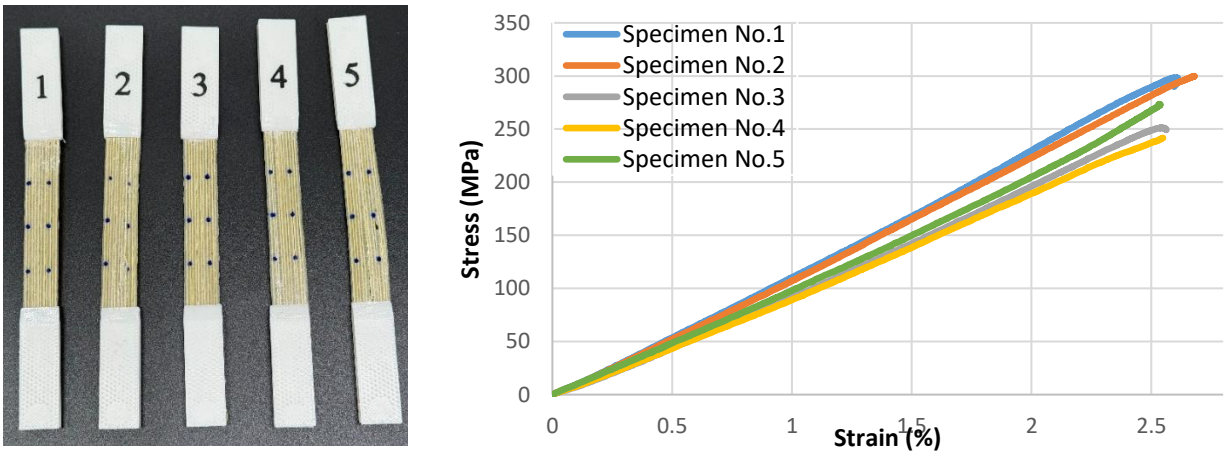

a b

Fig. 40. (PHBH/PBS)/AF composite results after tensile testing: a – broken composites, b – stress-strain curves

The results of (PHBH/PBS)/AF composites ranged from 244.39 to 299.97 MPa. Standard deviation and variation coefficient were 25.83 and 9.4%, respectively. These deviations are similar to those of (PHBH/PBS)/CF composites. These samples exhibited LIT and SIM failure modes, and they are classified as lateral inside tab failure mode at the top, and long splitting inside tab at the middle of the specimen, respectively. Also, composites reinforced with continuous aramid fibres after the tensile test did not break into two separate pieces, which was not the case with other types of composites.

3.3.3. Comparative Analysis of Tensile Results

Tensile strength results of all tested composite types are provided in Figure 41. It can be seen that glass fibre reinforcement provided the highest tensile strength and similar impact to both matrix materials. (PHBH/PBS)/GF composite type only had 1.7% higher tensile strength than the PHA/GF composite structures.

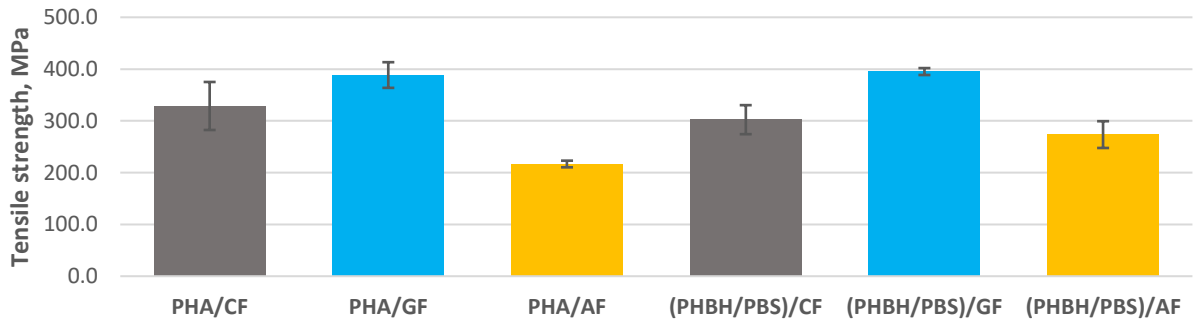

Fig. 41. Tensile strength results of all tested composite types

The results show that by reinforcing PHA polymer with carbon fibre it would have 8.7% higher tensile strength, on average, than (PHBH/PBS)/CF composite structure, and by reinforcing PHBH/PBS blend polymer with aramid fibre it would have 26.2% higher tensile strength, on average, than PHA/AF composite structure. Results also show that fibre contents in composite structures had a significant impact on tensile strengths. Young's modulus results of all tested composite types are provided in Figure 42.

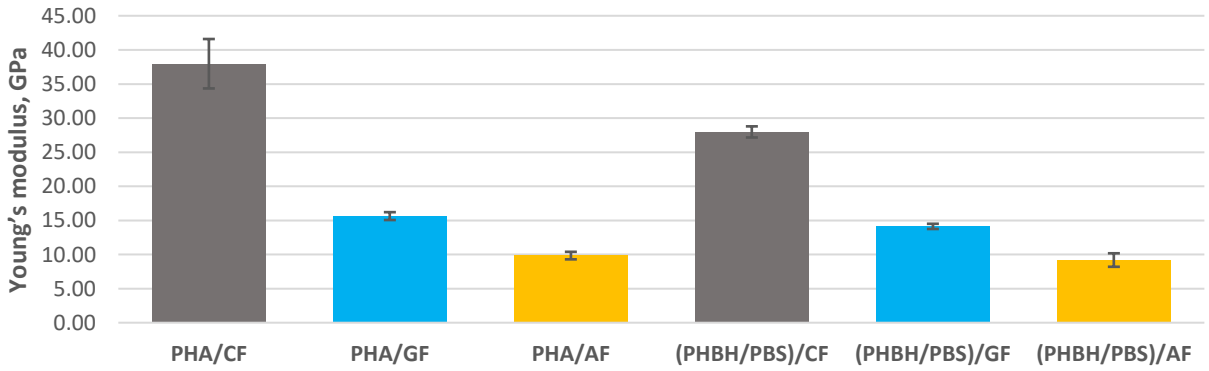

Fig. 42. Young's modulus results of all tested composite types

These results show that biopolymers reinforced with carbon fibre would have almost 2 times larger rigidity than those reinforced with glass or aramid fibres. Also, composites for which structure PHA was used as matrix material had slightly higher Young's modulus, for example PHA/CF, had 35.7% higher than (PHBH/PBS)/CF, PHA/GF, had 10.7% higher than (PHBH/PBS)/GF, and PHA/AF,

had 7.1% higher Young's modulus than (PHBH/PBS)/AF. For this comparison graph and results, the PHBH/PBS/CF specimen No. 1 test results were not included.

3.4. Results of Flexural Tests

3.4.1. Flexural Test Results of Composites Composed of PHA and Synthetic Fibres

A total of 15 composite specimens were printed with a PHA matrix for flexural testing (Fig. 43.): 5 specimens were reinforced with continuous carbon fibre towpreg (PHA/CF), 5 with continuous glass fibre towpreg (PHA/GF), and 5 with continuous aramid fibre towpreg (PHA/AF).

a b c

Fig. 43. Prepared composite flexural specimens: a – PHA/CF, b – PHA/GF, c – PHA/AF

The printed flexural specimens with PHA matrix after processing were weighed and measured. The weights, dimensions and calculated composite fibre, matrix and void contents are presented in Table 16.

Table 16. Dimensions, weights, and fibre, matrix, and void contents of a composite flexural specimen with a PHA matrix

Specimen type	S. No	Length, mm	Width, mm	Height, mm	Cross-sectional area, mm2	Weight, g	Fibre content, weight %	Matrix content, weight %	Void content, volume %
PHA/CF	1.	129.71	12.68	4.11	52.11	7.01	27.0%	73.0%	23.4%
	2.	128.69	12.57	4.05	50.91	6.73	27.9%	72.1%	24.3%
	3.	130.24	12.37	4.21	52.08	6.87	27.6%	72.4%	25.3%
	4.	129.63	12.54	4.09	51.29	6.91	27.4%	72.6%	23.3%
	5.	129.25	12.35	4.1	50.64	6.82	27.6%	72.4%	23.2%
	Average	**129.50**	**12.50**	**4.11**	**51.40**	**6.87**	**27.5%**	**72.5%**	**23.9%**
PHA/GF	1.	124.89	12.35	4.11	50.76	7.65	36.6%	63.4%	21.0%
	2.	125.64	12.09	4.09	49.45	7.67	36.7%	63.3%	19.2%
	3.	125.53	12.29	4.16	51.13	7.81	36.0%	64.0%	20.0%
	4.	124.46	12.17	4.12	50.14	7.74	36.0%	64.0%	18.5%
	5.	124.76	12.39	4.12	51.05	7.73	36.2%	63.8%	20.3%

Specimen type	S. No	Length, mm	Width, mm	Height, mm	Cross-sectional area, mm2	Weight, g	Fibre content, weight %	Matrix content, weight %	Void content, volume %
	Average	**125.06**	**12.26**	**4.12**	**50.50**	**7.72**	**36.3%**	**63.7%**	**19.8%**
PHA/AF	1.	124.59	11.21	3.99	44.73	5.53	13.9%	86.1%	21.5%
	2.	125.08	11.21	3.97	44.50	5.65	13.7%	86.3%	19.7%
	3.	124.56	11.25	3.97	44.66	5.57	13.8%	86.2%	20.8%
	4.	124.77	11.16	3.99	44.53	5.57	13.8%	86.2%	20.7%
	5.	124.77	11.18	4.01	44.83	5.52	13.9%	86.1%	22.0%
	Average	**124.75**	**11.20**	**3.99**	**44.65**	**5.57**	**13.8%**	**86.2%**	**20.9%**

The results show that the printed flexural specimens had a slightly smaller amount of fibre content weight than the tensile composite specimens. The analytically calculated density of these composites is 1.03 g/cm^3 of PHA/CF, 1.22 g/cm^3 of PHA/GF, and 1.00 g/cm^3 of PHA/AF on average. Overall, the PHA/GF composite had the highest analytical density, weight, and fibre content among other types of composites. The total void content volume of all composite types varies between 19.8% and 23.9%. These values are quite high, but are smaller than those of tensile specimens. The forces obtained during the flexural testing on composite flexural specimens with PHA matrix and the calculated flexural strength, along with flexural modulus, are presented in Table 17.

Table 17. Mechanical properties of composite flexural specimens with PHA matrix

Composite type	Specimen No.	Maximum force, N	Flexural strength, MPa	Flexural modulus, MPa
PHA/CF	1.	183	102.7	13565
	2.	191	111.4	15092
	3.	177	96.7	12265
	4.	205	117.3	14172
	5.	177	102.1	14184
	Average	**187±11.9**	**106.0±8.2**	**13856±1043**
PHA/GF	1.	167	95.9	8257
	2.	163	96.4	8222
	3.	169	95.2	7286
	4.	160	93.2	7990
	5.	166	94.6	7450
	Average	**165±3.3**	**95.1±1.2**	**7841±447.5**
PHA/AF	1.	85	57.2	3095
	2.	88	60.0	4868
	3.	90	60.9	4206
	4.	88	59.1	3856
	5.	83	55.1	3447
	Average	**87±2.9**	**58.4±2.3**	**3895±687**

The flexural results show that composite specimens, where PHA is reinforced with CF, had the highest flexural strength compared to those reinforced with other synthetic fibres. PHA/CF had the 106 MPa flexural strength, which is 11.5% higher than PHA/GF composites and 81.5% higher than PHA/AF composites flexural strengths, on average. Also, the PHA/CF composite type had the highest flexural modulus, meaning it was stiffer than other composite structures. PHA/CF composite structure type had 76.7% higher Young's modulus than the PHA/GF, and 255.7% higher than the PHA/AF composite type. Overall, composite structures reinforced with carbon and glass fibre exhibited better flexural properties than composites reinforced with aramid fibre. The PHA/CF composites after flexural testing and stress-strain curves are shown in Figure 44.

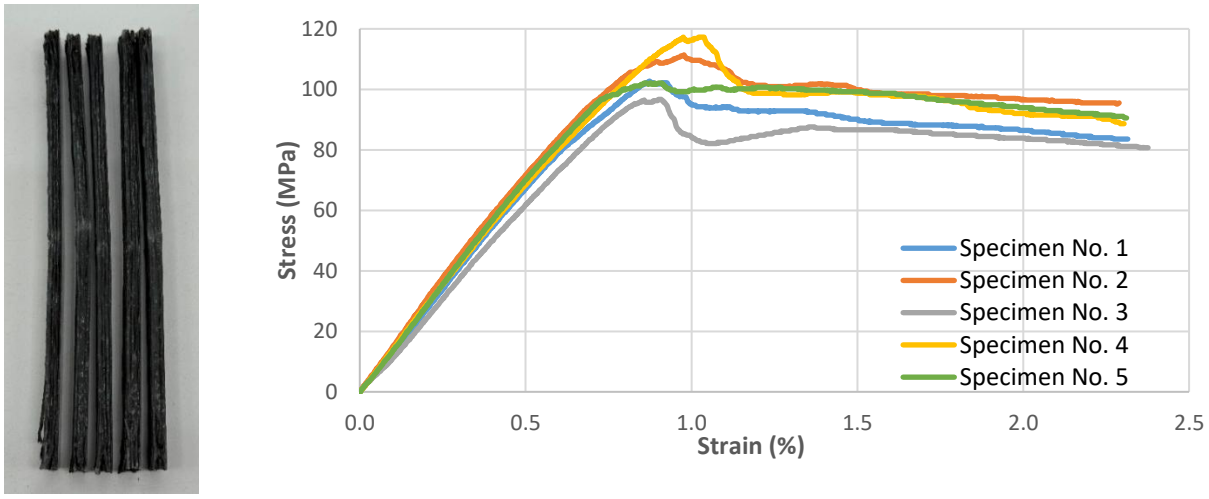

a b

Fig. 44. PHA/CF composite results after flexural testing: a – damaged composites, b – stress-strain curves

The flexural strength results of PHA/CF composites ranged from 96.7 to 117.3 MPa. Standard deviation and variation coefficient were 8.2 and 7.7%, respectively. From stress-strain curves, it can be seen that PHA/CF composites had a similar failure type. Moreover, these specimens showed no significant visual damage. The PHA/GF composites after flexural testing and stress-strain curves are shown in Figure 45.

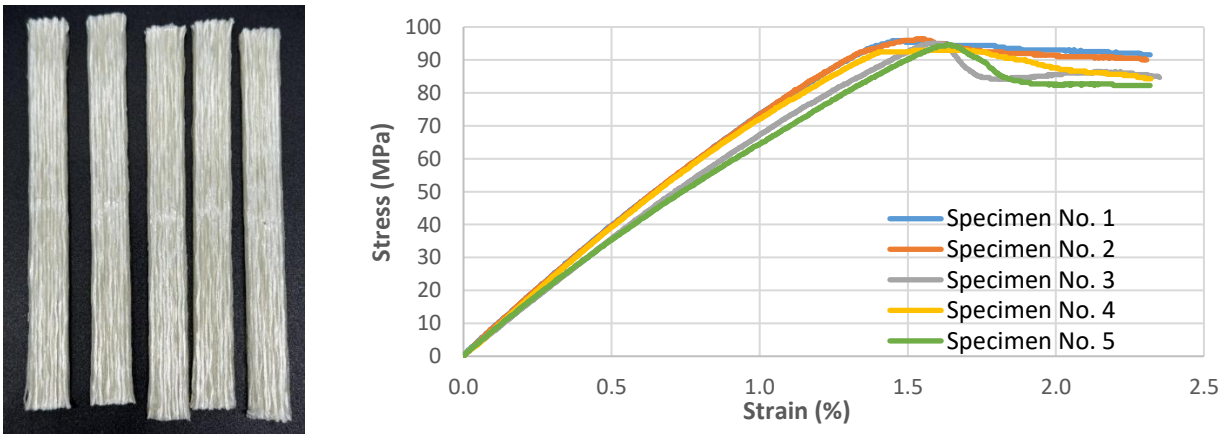

a b

Fig. 45. PHA/GF composite results after flexural testing: a – damaged composites, b – stress-strain curves

The flexural strength results of PHA/GF composites ranged from 93.2 to 96.4 MPa. Standard deviation and variation coefficient were 1.2 and 1.3%, respectively. From stress-strain curves, it can

be seen that PHA/GF composites had a similar failure type. Moreover, these specimens, after testing, were slightly damaged on the top surface. The PHA/AF composites after flexural testing and stress-strain curves are shown in Figure 46.

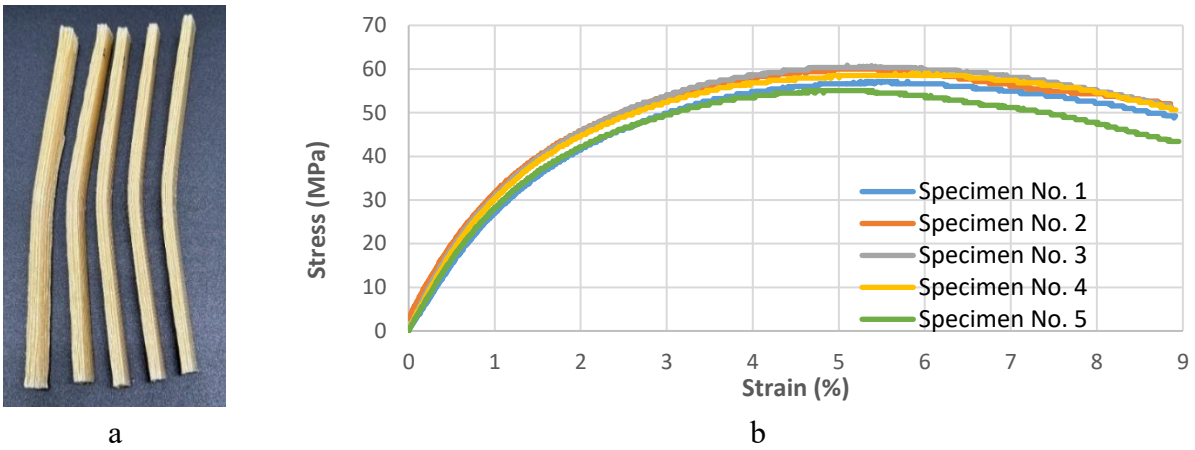

a b

Fig. 46. PHA/AF composite results after flexural testing: a – damaged composites, b – stress-strain curves

The flexural strength results of PHA/AF composites ranged from 55.1 to 60.9 MPa. Standard deviation and variation coefficient were 2.3 and 4%, respectively. From stress-strain curves, it can be seen that PHA/AF composites had high ductility, and all of them had similar results. Moreover, these specimens, after testing, were slightly deformed and did not have any visible damage.

3.4.2. Flexural Test Results of Composites Composed of PHBH/PBS and Synthetic Fibres

A total of 15 composite specimens were printed with a PHBH/PBS matrix for flexural testing (Fig. 47.): 5 specimens were reinforced with continuous carbon fibre towpreg ((PHBH/PBS)/CF), 5 with continuous glass fibre towpreg ((PHBH/PBS)/GF), and 5 with continuous aramid fibre towpreg ((PHBH/PBS)/AF).

a b c

Fig. 47. Prepared composite flexural specimens: a – (PHBH/PBS)/CF, b – (PHBH/PBS)//GF, c – (PHBH/PBS)//AF

The printed flexural specimens with the PHBH/PBS matrix after processing were weighed and measured. The weights, dimensions and calculated composite fibre, matrix and void contents are presented in Table 18.

Table 18. Dimensions, weights, and fibre, matrix, and void contents of a composite flexural specimen with a PHBH/PBS matrix

Specimen type	S. No	Length, mm	Width, mm	Height, mm	Cross-sectional area, mm2	Weight, g	Fibre content, weight %	Matrix content, weight %	Void content, volume %
(PHBH/PBS)/CF	1.	132.8	12.14	4.19	50.87	7.19	26.9%	73.1%	21.4%
	2.	132.77	12.08	4.21	50.86	7	27.7%	72.3%	23.6%
	3.	133.51	12.02	4.19	50.36	6.96	28.0%	72.0%	23.8%
	4.	132.14	12.03	4.16	50.04	6.73	28.6%	71.4%	25.2%
	5.	133.29	12.1	4.14	50.09	7.17	27.1%	72.9%	20.7%
	Average	**132.90**	**12.07**	**4.18**	**50.45**	**7.01**	**27.7%**	**72.3%**	**22.9%**
(PHBH/PBS)/GF	1.	136.02	11.41	4.03	45.98	7.42	41.1%	58.9%	24.5%
	2.	137.46	11.67	3.78	44.11	6.5	47.4%	52.6%	34.6%
	3.	137.02	11.43	3.99	45.61	7.32	41.9%	58.1%	25.9%
	4.	136.1	12.02	4.12	49.52	8.28	36.8%	63.2%	19.7%
	5.	136.68	12.09	4.12	49.81	8.06	38.0%	62.0%	23.2%
	Average	**136.66**	**11.72**	**4.01**	**47.01**	**7.52**	**41.0%**	**59.0%**	**25.6%**
(PHBH/PBS)/AF	1.	132.54	10.72	4.06	43.52	5.85	14.0%	86.0%	19.8%
	2.	131.73	10.76	4.07	43.79	5.66	14.4%	85.6%	22.5%
	3.	131.99	10.81	3.96	42.81	5.23	15.6%	84.4%	27.0%
	4.	132.99	10.76	4.07	43.79	5.6	14.7%	85.3%	24.0%
	5.	134.36	10.81	4.07	44.00	5.87	14.1%	85.9%	21.5%
	Average	**132.72**	**10.77**	**4.05**	**43.58**	**5.64**	**14.5%**	**85.5%**	**23.0%**

The results show that the printed flexural specimens with PHBH/PBS blend matrix had a slightly smaller amount of fibre weight than the tensile composite specimens. Overall, flexural specimens reinforced with CF had 27.6% of fibre content, with GF had 38.7%, and with AF 14.2%, which are lower than tensile specimens, because of different printing parameters. The analytically calculated density of these composites is 1.05 g/cm3 of (PHBH/PBS)/CF, 1.17 g/cm3 of (PHBH/PBS)/GF, and 0.98 g/cm3 of (PHBH/PBS)/AF on average. Overall, the (PHBH/PBS)/GF composite had the highest analytical density, weight, and fibre content among other types of composites. The total void content volume of all composite types varies between 22.9% and 25.6%. (PHBH/PBS)/GF specimen No. 2 was printed with the lowest matrix content and highest void content among other (PHBH/PBS) GF specimens. The forces obtained during the flexural testing on composite flexural specimens with PHBH/PBS blend matrix and the calculated flexural strength, along with flexural modulus, are presented in Table 19.

Table 19. Mechanical properties of composite flexural specimens with PHBH/PBS matrix

Composite type	Specimen No.	Maximum force, N	Flexural strength, MPa	Flexural modulus, MPa
(PHBH/PBS)/CF	1.	161	90.6	11660
	2.	146	81.7	10652

Composite type	Specimen No.	Maximum force, N	Flexural strength, MPa	Flexural modulus, MPa
	3.	138	78.2	11149
	4.	128	74.0	10238
	5.	146	84.4	11850
	Average	**144±12**	**81.8±6.3**	**11110±675**
(PHBH/PBS)/GF	1.	94	60.6	5512
	2.	42	30.0	2615
	3.	87	57.2	5112
	4.	138	80.9	6994
	5.	130	76.0	6167
	Average	**98±38.4**	**60.9±20**	**5280±1651.6**
(PHBH/PBS)/AF	1.	84	57.2	2984
	2.	80	53.9	2735
	3.	51	36.0	2444
	4.	74	49.9	2565
	5.	88	59.0	3335
	Average	**75±14.7**	**51.2±9.2**	**2813±355.4**

The flexural results show that composite specimens, where PHBH/PBS is reinforced with CF, had the highest flexural strength compared to those reinforced with other synthetic fibres. (PHBH/PBS)/CF had the 81.8 MPa flexural strength, which is 33.1% higher than (PHBH/PBS)/GF composites, and 59.8% higher than (PHBH/PBS)/AF composites flexural strengths, on average. Also, the (PHBH/PBS)/CF composite type had the highest flexural modulus, meaning it was stiffer than other composite structures. (PHBH/PBS)/CF composite structure type had 110.4% higher Young's modulus than the (PHBH/PBS)/GF, and 294.5% higher than the (PHBH/PBS)/AF composite type. Overall, composite structures reinforced with carbon and glass fibre exhibited better flexural properties than composites reinforced with aramid fibre. The (PHBH/PBS)/CF composites after flexural testing and stress-strain curves are shown in Figure 48.

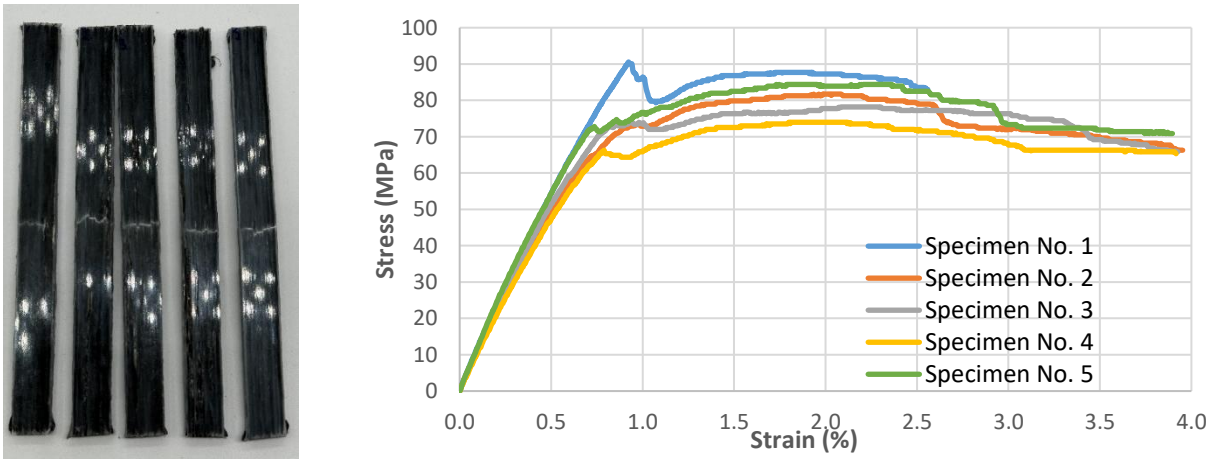

a b

Fig. 48. (PHBH/PBS)/CF composite results after flexural testing: a – damaged composites, b – stress-strain curves

The flexural strength results of (PHBH/PBS)/CF composites ranged from 74 to 90.6 MPa. Standard deviation and variation coefficient were 6.3 and 7.7%, respectively. From stress-strain curves, it can be seen that (PHBH/PBS)/CF composites had a similar failure type. Moreover, these specimens had a crack at the bottom of the specimens. The (PHBH/PBS)/GF composites after flexural testing and stress-strain curves are shown in Figure 49.

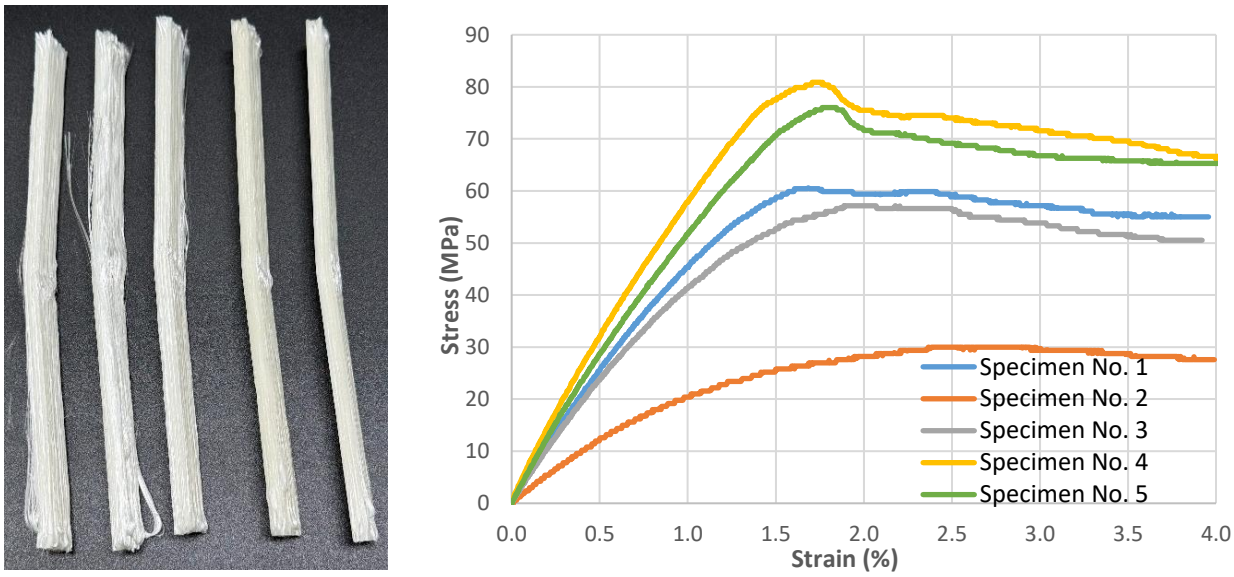

a b

Fig. 49. (PHBH/PBS)/GF composite results after flexural testing: a – damaged composites, b – stress-strain curves

The flexural strength results of (PHBH/PBS)/GF composites ranged from 30 to 80.9 MPa. Standard deviation and variation coefficient were 20 and 32.8%, respectively. This wide variation in results was due to the specimen No. 2, which was produced with a smaller amount of matrix material than the other specimens. By excluding the results of specimen No. 2 from stress-strain curves, it can be concluded that (PHBH/PBS)/GF composites had a similar failure type. Moreover, these specimens mostly had a slight crack at the bottom of the specimen. The (PHBH/PBS)/AF composites after flexural testing and stress-strain curves are shown in Figure 50.

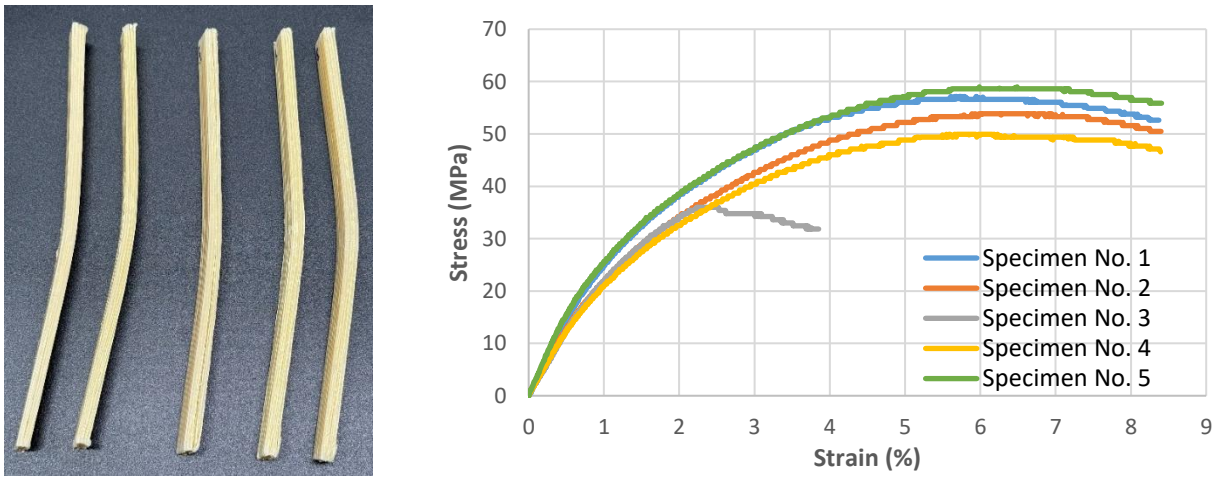

a b

Fig. 50. (PHBH/PBS)/AF composite results after flexural testing: a – damaged composites, b – stress-strain curves

The flexural strength results of (PHBH/PBS)/AF composites ranged from 36 to 57.2 MPa. Standard deviation and variation coefficient were 9.2 and 17.9%, respectively. This wide variation in results was due to the specimen No. 3, and this was influenced by poor IFSS between the PHBH/PBS matrix and AF towpreg. From stress-strain curves, it can be seen that (PHBH/PBS)/AF composites had high ductility and almost all of them had similar results, except the specimen No. 3, which had an interlaminar shear failure mode, while other specimens after testing were only slightly deformed and did not have any visible damage.

3.4.3. Comparative Analysis of Flexural Results

Flexural strength results of all tested composite types are provided in Figure 51. It can be seen that carbon fibre reinforcement has provided the highest flexural strength to both matrix materials. In the provided comparison graphs, the results of (PHBH/PBS)/GF specimen No. 2 and (PHBH/PBS)/AF specimen No. 3 were not included.

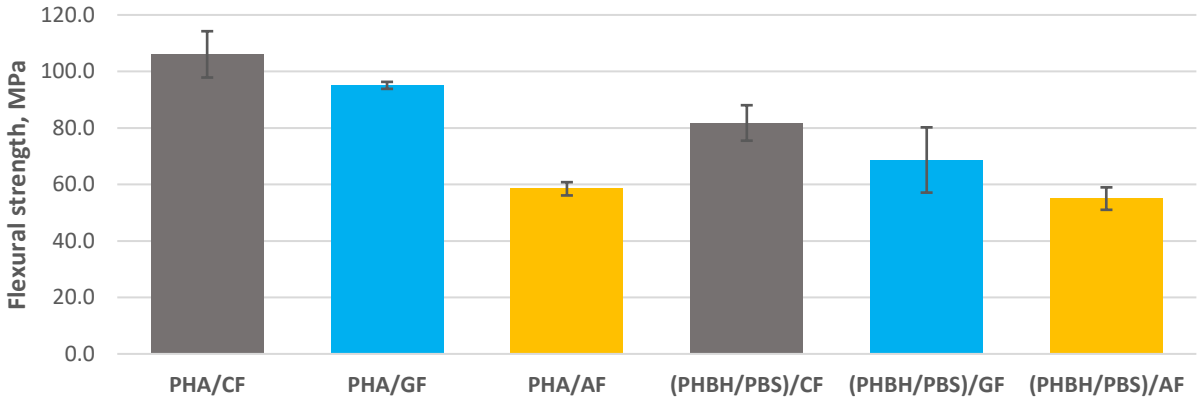

Fig. 51. Flexural strength results of all tested composite types

The results show that by reinforcing PHA polymer with synthetic fibre it would have higher flexural strength than composites for which the PHBH/PBS polymer is used. For example, PHA/CF had 29.6% higher flexural strength than (PHBH/PBS)/CF, PHA/GF had 38.5% higher flexural strength than (PHBH/PBS)/GF, and PHA/AF had 6.2% higher flexural strength than (PHBH/PBS)/AF. Flexural modulus results of all tested composite types are provided in Figure 52.

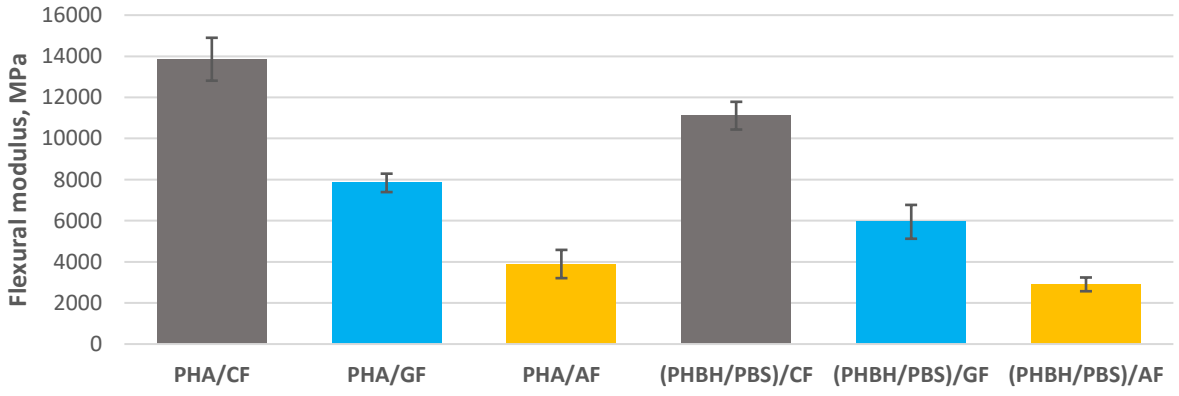

Fig. 52. Flexural modulus results of all tested composite types

These results, similarly as tensile results, show that biopolymers reinforced with carbon fibre would have almost 2 times larger rigidity than reinforced with glass or aramid fibres. Also, composites for

which structure PHA was used as matrix material had slightly higher flexural modulus, for example, PHA/CF had 24.7% higher than (PHBH/PBS)/CF, PHA/GF had 31.9% higher than (PHBH/PBS)/GF, and PHA/AF had 38.5% higher than (PHBH/PBS)/AF.

3.5. Chapter Summary

This chapter covers resin content calculation of impregnated synthetic fibres, which helped to determine the quality of prepared towpregs, and interfacial shear strength test results of unimpregnated and impregnated synthetic fibres with different polymer matrix materials, which showed compatibility of synthetic fibres with biopolymers and the impact of impregnation for IFSS improvement. Additionally, this section covers additive manufacturing processes of tensile and flexural test composite specimens and the challenges posed by the materials used. It also provides the dimensions of the produced specimens, the calculated contents of reinforcing fibre, and air voids in the composite specimens, and an analysis of the mechanical properties of the composite specimens. The resin calculations have shown that it is difficult to properly impregnate synthetic fibres with PHBH/PBS biopolymer by using the melt impregnation method, and that each synthetic fibre type brings different processing challenges. IFSS test results have shown that unimpregnated synthetic fibres are more compatible with the PHBH/PBS blend biopolymer than with the PHA matrix by 39%, on average. Also, pull-out test results have shown that synthetic fibre impregnation improved IFSS with PHA by 53.9%, and with PHBH/PBS by 26.2 %, on average. Moreover, during the printing process of composite structures, it was noted that by using PHBH/PBS as the matrix material, the production process is less complicated than using PHA. Also, mechanical properties test results have shown that fibre content in the composite significantly impacts tensile strength, and fibre type impacts the composite structures rigidity. For example, composite structures reinforced with the highest glass fibre content exhibited the highest tensile strength, while carbon fibre reinforced composites had the highest Young's modulus, flexural strength and modulus. By reinforcing biopolymers with aramid fibre it was noted that composite structures would not be as resistant to high tensile and flexural loadings as other synthetic fibres, but would have more flexibility and ductility.

4. Composite Specimens Production Cost

Traditional composite production is quite expensive since it requires manual labour, many tools, and lots of materials are wasted producing small parts. Therefore, by applying additive manufacturing, some expenses can be avoided, because less waste is generated, less expensive equipment is used, and an automated or semi-automated process, for which skilled personnel are not required. Furthermore, the number of parts produced does not affect the cost of production.

4.1. Towpreg Preparation Cost

Impregnated fibres were used to produce the composite specimens in this study. The use of towpregs increased the cost of producing the final composite structures. To estimate the cost of impregnation, material costs were calculated, and the cost of custom melt impregnation equipment was added to the cost calculation. The used equipment consisted of a direct drive extruder with a modified impregnation chamber, which costs roughly 170 Eur [76], a stepper motor, whose price is around 30 Eur [77], and other electronics, such as power supplies, control units, and sensors, which could add up to 100 Eur to the equipment cost. All things combined, it can be estimated that the price of the impregnation equipment is around 300 Eur. Also, it can be estimated that this equipment consumes 100W of power during the impregnation process. To calculate the impregnated towpreg cost, the following formula was used:

$$Syntehtic\ towpreg\ cost\ (Eur/m) = \frac{EHR+UMHR}{M_{ph}} \quad (14)$$

where EHR – equipment hourly rate, UHMR – used materials hourly rate cost (Eur/h), M_{ph} – meters per hour (depends on parameters, the amount of fibre in meters impregnated per hour).

4.1.1. Material Consumption During Towpreg Production

During this study, 3 types of synthetic fibres were impregnated with a PHBH/PBS mixture biopolymer. The cost and consumption of these materials are calculated in towpregs cost. It was given that the price of 3K CF tow is 0.03 Eur/m on average [78], the price of GF tow is 0.003 Eur/m, and the price of AF tow is 0.014 Eur/m [79]. PHBH/PBS blend filament was used in the impregnation process. It is known that this material has a density of 1.24 g/cm^3, and this blend is composed of PHBH and PBS polymers. 1 kg of PHBH pellets costs 48.40 Eur [80], and 1 kg of PBS powder costs 50.95 Eur [81]. This means that the PHBH/PBS filaments price would be 49.68 Eur/kg. Biopolymer consumption was calculated based on the impregnation parameters. PHBH/PBS filament was fed into the heating block at a speed of 12 mm/min, and fibre was pulled through it at a 1200 mm/min linear speed. Knowing that the diameter of the filament is 1.75 mm, the volume and mass flow of the filament were calculated using the following formulas:

$$A = \pi r^2 = \pi * \left(\frac{0.175}{2}\right)^2 = 0.024\ cm^2 \quad (15)$$

$$V_{FR} = A * FR = 0.024(cm^2) * 1.2\ (cm/min) = 0.029\ cm^3/min \quad (16)$$

$$M_{FR} = V_{FR} * Denisty = 0.029\ (cm^3/min) * 1.24(g/cm^3) = 0.036\ g/min \quad (17)$$

where V_{FR} – volume flow rate, and M_{FR} – material flow rate. It was calculated that the mass flow rate into the extruder is 0.036 g/min, and 1200 mm of fibre is pulled in a minute. Then, 0.03g of

PHBH/PBS blend polymer is used to impregnate 1 meter of synthetic fibre. Over one hour of the impregnation process, only 1.8 g of matrix material is used, which costs only 0.09 Eur.

Also, in one hour, 72 meters (M_{ph}) of fibre tow is impregnated, therefore the cost of synthetic fibre accounts for a larger portion of the expense. The cost of used synthetic fibres and matrix in one hour is shown in the following calculations:

$$UHMR_{CF} = S_m + S_{CF} = 0.09(Eur) + \big(72 * 0.03(Eur/m)\big) = 2.25\ Eur/h \quad (18)$$

$$UHMR_{GF} = S_m + S_{AF} = 0.09(Eur) + \big(72 * 0.003(Eur/m)\big) = 0.31\ Eur/h \quad (19)$$

$$UHMR_{AF} = S_m + S_{AF} = 0.09(Eur) + \big(72 * 0.014(Eur/m)\big) = 1.1\ Eur/h \quad (20)$$

where UHMR – used materials hourly rate cost, Eur/h; CF – carbon fibre; GF – glass fibre; AF – aramid fibre; S_m – cost of used matrix per hour. Calculations show that using carbon fibre instead of glass fibre can increase the cost of the materials by a factor of 10.

4.1.2. Impregnation Equipment Cost Impact on the Price of the Towpreg

The impregnation equipment consumes 0.1 kWh per hour, which costs approximately 0.022 Eur/h. Considering that the impregnation process is automated, but requires starting and stopping, which would take 5 minutes of manual labour, the cost of completion of this task may be evaluated at 0.8 Eur. However, even if the impregnation process is not complete after one hour, it can be considered as a routine inspection of the equipment, which can be carried out at regular intervals and may be performed by human resources. The depreciation of the equipment can be calculated based on its service life, which is estimated to be enough to impregnate 100 kilometres of fibre. In this case, the cost of impregnating one meter of fibre would be 0.003 EUR, and the hourly depreciation would be 0.22 EUR. Equipment's hourly rate was calculated using the following formula:

$$EHR = S_{ene} + S_{dep} + S_{per} = 0.022 + 0.216 + 0.8 = 1.038\ Eur/h \quad (21)$$

where S_{ene} – hourly energy consumption cost, Eur/h; S_{dep} – hourly depreciation cost of the equipment, Eur/h; and S_{per} – hourly employee labour cost related to the equipment operation, Eur/h. Lastly, the towpreg cost of one meter for each fibre type was calculated using the following formulas:

$$CF\ towpreg\ cost = \frac{EHR + UHMR_{CF}}{M_{ph}} = \frac{1.038 + 2.25}{72} = 0.046\ Eur/m \quad (22)$$

$$GF\ towpreg\ cost = \frac{EHR + UHMR_{GF}}{M_{ph}} = \frac{1.038 + 0.31}{72} = 0.019\ Eur/m \quad (23)$$

$$AF\ towpreg\ cost = \frac{EHR + UHMR_{AF}}{M_{ph}} = \frac{1.038 + 1.1}{72} = 0.03\ Eur/m \quad (24)$$

4.2. Composite Structures Production Cost

Composite manufacturing costs are calculated by taking into account the materials used, the hourly rate of machinery, which involves electricity usage and printer depreciation, and also additional cost which is associated with the setup of equipment and parts removal from the build plate. Printing cost was calculated using the following formula:

$$Printing\ cost = Material\ cost + MHR * Prduction\ time + Setup\ cost \quad (25)$$

4.2.1. Cost of Materials used for Printing

The cost of the materials used varied depending on the type of matrix and type of fibre, while the materials used depended only on the type of specimen, whether it is a tensile or bending specimen.

PHA filaments 1 kg cost about 29.67 Eur [82], and PHBH/PBS blend filament costs 49.68 Eur/kg. To produce tensile specimens, 1.2 g of filament was used and to produce flexural specimens, 4.9 g of filament was used for each specimen structure. Therefore, by applying the material consumption formula, the matrix material usage to produce each specimen was calculated:

$$Cost = \frac{Matrix\ material\ usage\ (g)}{1000} + Filament\ price\ (Eur/kg) \quad (26)$$

- PHA material cost to produce tensile test composite: 0.04 Eur
- PHBH/PBS material cost to produce tensile test composite: 0.06 Eur
- PHA material cost to produce flexural test composite: 0.15 Eur
- PHBH/PBS material cost to produce flexural test composite: 0.24 Eur

Towpreg usage cost in composite production is calculated based on the amount of synthetic fibres used to reinforce these composite structures. For tensile test specimens, 3.3 meters of synthetic towpregs were used, and for flexural test specimens, 10.8 meters of synthetic towpregs were used. Calculated cost of towpreg used per composite type:

- CF in tensile specimens: 3.3*0.046=0.15 Eur
- GF in tensile specimens: 3.3*0.019=0.06 Eur
- AF in tensile specimens: 3.3*0.03=0.1 Eur
- CF in flexural specimens: 10.8*0.046=0.5 Eur
- GF in flexural specimens: 10.8*0.019=0.21 Eur
- AF in flexural specimens: 10.8*0.03=0.33 Eur

4.2.2. Composite Specimens Production Cost, Including Setup and Equipment Cost

The equipment hourly rate is calculated, including printer depreciation and energy consumption. The used printer costs around 424 Eur [83]. If a custom printhead, which costs about 150 Eur approximately, is added to the equipment price, then the printer price is worth 574 Eur. The typical service life of such a printer is approximately 8 years. If it is estimated that the printer will work 2000 hours per day, then the depreciation cost of the machine:

$$S_{dep} = \frac{574}{8*2000} = 0.036\ Eur/h \quad (27)$$

To fully calculate the printer hourly rate, electricity consumption needs to be estimated. The printer consumes around 0.2 kWh during normal printing, and the electricity price is 0.22 EUR/kWh. Therefore, the energy cost is 0.044 Eur/h. Knowing the equipment hourly depreciation and energy consumption, the machnies hourly rate was calculated:

$$MHR = S_{dep} + S_{ele} = 0.036 + 0.044 = 0.08\ Eur/h \quad (28)$$

If labour cost is included in the production of composites, then an additional 0.8 Eur of machine setup cost can be added for each specimen type. To produce a tensile specimen, it takes about 25 minutes, and to produce a flexural specimen, it takes about 95 minutes of production time. Composite

production costs for each specimen type, excluding material costs, were calculated using the following formula:

$$Specimen\ production\ cost = MHR * Production\ time + Setup \quad (28)$$

- Tensile specimen production cost=0.08*0.42+0.8=0.84 Eur
- Flexural specimen production cost==0.08*1.6+0.8=0.93 Eur

These specimen production costs were added to the material consumption, and the total composite specimen production costs were recalculated for their type and the composed materials types, using the following formula:

$$Total\ production\ cost = MC_M + MC_F + Specimen\ production\ cost \quad (29)$$

Where MC_M – matrix material consumption cost, MC_F – towpreg material consumption cost.

- Total PHA/CF tensile composite production cost: 0.04+0.15+0.84=**1.03 Eur**
- Total PHA/GF tensile composite production cost: 0.04+0.06+0.84=**0.94 Eur**
- Total PHA/AF tensile composite production cost: 0.04+0.1+0.84=**0.98 Eur**
- Total (PHBH/PBS)/CF tensile composite production cost: 0.06+0.15+0.84=**1.05 Eur**
- Total (PHBH/PBS)//GF tensile composite production cost: 0.06+0.06+0.84=**0.96 Eur**
- Total (PHBH/PBS)//AF tensile composite production cost: 0.06+0.1+0.84=**1 Eur**
- Total PHA/CF flexural composite production cost: 0.15+0.5+0.93=**1.58 Eur**
- Total PHA/GF flexural composite production cost: 0.15+0.21+0.93=**1.29 Eur**
- Total PHA/AF flexural composite production cost: 0.15+0.33+0.93=**1.41 Eur**
- Total (PHBH/PBS)/CF flexural composite production cost: 0.24+0.5+0.93=**1.67 Eur**
- Total (PHBH/PBS)//GF flexural composite production cost: 0.24+0.21+0.93= **1.38 Eur**
- Total (PHBH/PBS)//AF flexural composite production cost: 0.24+0.33+0.93=**1.5 Eur**

From the calculations provided, it can be seen that the costs of raw materials, electricity and equipment do not have a significant impact on the price of the composite, as the main factor affecting the price is the cost of labour. Therefore, when producing larger samples, their price did not increase as significantly. For example, PHA/CF tensile composite materials account for 18.4% of the total cost of the sample, while flexural composite materials account for 41.1% of the total cost of the sample.

4.3. Chapter Summary

This chapter covers the production cost of the additively manufactured composite structures. The towpreg preparation cost calculation is provided, during which it was calculated that to melt impregnated carbon fibre with PHBH/PBS polymer costs 0.046 Eur per meter, and other synthetic fibres, such as glass fibre it costs 0.019 Eur per meter, and aramid fibre 0.03 Eur per meter. The costs of the manufactured composite specimens were also calculated. It was calculated that producing one tensile specimen costs an average of 0.99 Eur, while a flexural test specimen production costs 1.47 Eur on average.

Conclusions

1. Synthetic fibres impregnation was performed with PHBH/PBS blend biopolymer before AM process to achieve better bonding between the matrix and reinforcement material. CF towpregs were prepared with 24.6% RC content, GF with 15%, and AF with 34.4%. Pull-out test results have shown that fibre impregnation improves IFSS with PHA by 53.9%, and with PHBH/PBS by 26.2 %, on average. Only the aramid fibres interface with PHBH/PBS was decreased after impregnation.
2. Composite structure specimens composed of biopolymers and synthetic fibres were prepared by applying material extrusion and towpreg co-extrusion methods. During production, it was observed that the printing process is less complicated when using PHBH/PBS as a matrix material rather than PHA.
3. Reinforcement material content in prepared composite structure evaluated in accordance with ASTM D2734 standard. It was determined that tensile specimens reinforced with CF had 32.7% of fibre content, with GF had 44.7%, and with AF 17.2%. Also, flexural specimens reinforced with CF had 27.6% of fibre content, with GF had 38.7%, and with AF 14.2%, which were lower than tensile specimens, because of different printing parameters. These reinforcement contents significantly impacted the mechanical properties of composite structures.
4. Tensile and flexural mechanical test results determined that PHA/CF composite structures had the highest Young's modulus and flexural properties, compared to other composite structure types. These structures exhibited a tensile strength of 328.7 MPa, Young's modulus of 37.97 GPa, flexural strength of 106 MPa, and flexural modulus of 13.86 GPa. The highest tensile strength was achieved with (PHBH/PBS)/GF composite structures, which had 395.2 MPa of tensile strength. PHBH/PBS)/AF composite structures had the poorest mechanical properties, which were 273.5 MPa of tensile strength, 9.19 GPa of Young's modulus, 51.2 MPa of flexural strength, and 2.8 GPa of flexural modulus. Also, composites reinforced with AF had a more flexible and ductile structure than biopolymers with CF or GF reinforcements.

List of References

1. STOIMENOV, N., KOTSEVA, G. and GEORGIEVA, V. *Classification of 3d Print Technologies.* May 27, 2025. DOI 10.53656/adpe-2025.04.
2. ISO/ASTM 52900:2021(En), Additive Manufacturing — General Principles — Fundamentals and Vocabulary. [viewed Mar 1, 2026]. Available from: https://www.iso.org/obp/ui/#iso:std:iso-astm:52900:ed-2:v1:en.
3. CHENG, P., et al. 3D Printed Continuous Fibre Reinforced Composite Lightweight Structures: A Review and Outlook. *Composites Part B: Engineering*, -02-01, 2023, vol. 250. pp. 110450. ISSN 1359-8368. DOI 10.1016/j.compositesb.2022.110450.
4. LU, Y. and OZCAN, S. Green Nanomaterials: On Track for a Sustainable Future. *Nano Today*, -08-01, 2015, vol. 10, no. 4. pp. 417–420. ISSN 1748-0132. DOI 10.1016/j.nantod.2015.04.010.
5. FLÓREZ, M., CAZÓN, P. and VÁZQUEZ, M. Selected Biopolymers' Processing and their Applications: A Review. *Polymers*, /1, 2023, vol. 15, no. 3. pp. 641. ISSN 2073-4360. DOI 10.3390/polym15030641.
6. PÉREZ, M., CAROU, D., RUBIO, E. and TETI, R. Current Advances in Additive Manufacturing. *Procedia CIRP*, June 1, 2020, vol. 88. pp. 439–444. DOI 10.1016/j.procir.2020.05.076.
7. YUAN, S., LI, S., ZHU, J. and TANG, Y. Additive Manufacturing of Polymeric Composites from Material Processing to Structural Design. *Composites Part B: Engineering*, -08-15, 2021, vol. 219. pp. 108903. ISSN 1359-8368. DOI 10.1016/j.compositesb.2021.108903.
8. NARTU, M.S.K.K.Y. and AGRAWAL, P. Additive Manufacturing of Metal Matrix Composites. *Materials & Design*, -04-01, 2025, vol. 252. pp. 113609. ISSN 0264-1275. DOI 10.1016/j.matdes.2025.113609.
9. ZIAEE, M. and CRANE, N.B. Binder Jetting: A Review of Process, Materials, and Methods. *Additive Manufacturing*, -08-01, 2019, vol. 28. pp. 781–801. ISSN 2214-8604. DOI 10.1016/j.addma.2019.05.031.
10. KHAN, F., et al. Fabrication of SiC–Aluminum Composites Via Binder Jetting 3D Printing and Infiltration: A Feasibility Study. *Journal of Composites Science*, /3, 2025, vol. 9, no. 3. pp. 111. ISSN 2504-477X. DOI 10.3390/jcs9030111.
11. LV, X., et al. Binder Jetting Additive Manufacturing of Hierarchical Structural SiCw/SiC Composites. *Additive Manufacturing*, -08-05, 2024, vol. 93. pp. 104434. ISSN 2214-8604. DOI 10.1016/j.addma.2024.104434.
12. CHO, K.T., NUNEZ, L., SHELTON, J. and SCIAMMARELLA, F. Investigation of Effect of Processing Parameters for Direct Energy Deposition Additive Manufacturing Technologies. *Journal of Manufacturing and Materials Processing*, /6, 2023, vol. 7, no. 3. pp. 105. ISSN 2504-4494. DOI 10.3390/jmmp7030105.
13. FEENSTRA, D.R., et al. Critical Review of the State of the Art in Multi-Material Fabrication Via Directed Energy Deposition. *Current Opinion in Solid State and Materials Science*, -08-01, 2021, vol. 25, no. 4. pp. 100924. ISSN 1359-0286. DOI 10.1016/j.cossms.2021.100924.
14. KELLY, J.P., et al. Directed Energy Deposition Additive Manufacturing of Functionally Graded Al-W Composites. *Additive Manufacturing*, -03-01, 2021, vol. 39. pp. 101845. ISSN 2214-8604. DOI 10.1016/j.addma.2021.101845.

15. SVETLIZKY, D., et al. Directed Energy Deposition (DED) Additive Manufacturing: Physical Characteristics, Defects, Challenges and Applications. *Materials Today*, -10-01, 2021, vol. 49. pp. 271–295. ISSN 1369-7021. DOI 10.1016/j.mattod.2021.03.020.
16. PETRAT, Torsten; BRUNNER-SCHWER, C.; GRAF, Benjamin and RETHMEIER, Michael. Microstructure of Inconel 718 parts with constant mass energy input manufactured with direct energy deposition. *Procedia Manufacturing*, vol. 36 (2019), pp. 256–266. Available from: https://www.researchgate.net/publication/335419536_Microstructure_of_Inconel_718_parts_with_constant_mass_energy_input_manufactured_with_direct_energy_deposition.
17. SUN, X., MAZUR, M. and CHENG, C. A Review of Void Reduction Strategies in Material Extrusion-Based Additive Manufacturing. *Additive Manufacturing*, -04-05, 2023, vol. 67. pp. 103463. ISSN 2214-8604. DOI 10.1016/j.addma.2023.103463.
18. SELVAKANNAN, P., MAZUR, M. and SUN, X. Additive Manufacturing for Chemical Sciences and Engineering S.K. BHARGAVA, S. RAMAKRISHNA, M. BRANDT and P. SELVAKANNAN eds., Singapore: Springer Nature, 2022. *Material Extrusion and Vat Photopolymerization—Principles, Opportunities and Challenges*, pp. 53–76. ISBN 9789811922930.
19. YANG, Z., YANG, Z., CHEN, H. and YAN, W. 3D Printing of Short Fibre Reinforced Composites Via Material Extrusion: Fibre Breakage. *Additive Manufacturing*, -10-01, 2022, vol. 58. pp. 103067. ISSN 2214-8604. DOI 10.1016/j.addma.2022.103067.
20. ELKASEER, A., et al. Material Jetting for Advanced Applications: A State-of-the-Art Review, Gaps and Future Directions. *Additive Manufacturing*, -12-01, 2022, vol. 60. pp. 103270. ISSN 2214-8604. DOI 10.1016/j.addma.2022.103270.
21. GÜLCAN, O., GÜNAYDIN, K. and TAMER, A. The State of the Art of Material Jetting—A Critical Review. *Polymers*, /1, 2021, vol. 13, no. 16. pp. 2829. ISSN 2073-4360. DOI 10.3390/polym13162829.
22. Material jetting*In: Polymers for 3D Printing*, pp. 91–103William Andrew Publishing, 2022. Available from: https://www.sciencedirect.com/science/chapter/edited-volume/pii/B9780128183113000227.
23. DEJENE, N.D. and LEMU, H.G. Current Status and Challenges of Powder Bed Fusion-Based Metal Additive Manufacturing: Literature Review. *Metals*, /2, 2023, vol. 13, no. 2. ISSN 2075-4701. DOI 10.3390/met13020424.
24. Powder Bed Fusion in 3D Printing: Pros and Cons - EBM MACHINE [viewed Mar 1, 2026]. Available from: https://ebeammachine.com/powder-bed-fusion-in-3d-printing-pros-and-cons/.
25. PILIPOVIĆ, A. Polymers for 3D Printing J. IZDEBSKA-PODSIADŁY ed., William Andrew Publishing, 2022 *Chapter 11 - Sheet Lamination*, pp. 127–136. ISBN 9780128183113. DOI 10.1016/B978-0-12-818311-3.00008-2.
26. KUMAR, A., DIXIT, A.R. and SREENIVASA, S. Mechanical Properties of Additively Manufactured Polymeric Composites using Sheet Lamination Technique and Fused Deposition Modeling: A Review. *Polymers for Advanced Technologies*, 2024, vol. 35, no. 4. pp. e6396. ISSN 1042-7147. DOI 10.1002/pat.6396.
27. Sensing Materials: Electrochemical Sensors Enabled by 3D Printing (2023), pp. 73–88. Available from: https://www.sciencedirect.com/science/chapter/referencework/pii/B9780128225486000212.

28. LI, Y., WANG, W., WU, F. and KANKALA, R.K. Vat Polymerization-Based 3D Printing of Nanocomposites: A Mini Review. *Frontiers in Materials*, -01-05, 2023, vol. 9. ISSN 2296-8016. DOI 10.3389/fmats.2022.1118943.
29. LEE, H., et al. Effect of Different Vat Polymerization Techniques on Mechanical and Biological Properties of 3D-Printed Denture Base. *Polymers*, /1, 2023, vol. 15, no. 6. pp. 1463. ISSN 2073-4360. DOI 10.3390/polym15061463.
30. PAGAC, M., et al. A Review of Vat Photopolymerization Technology: Materials, Applications, Challenges, and Future Trends of 3D Printing. *Polymers*, /1, 2021, vol. 13, no. 4. pp. 598. ISSN 2073-4360. DOI 10.3390/polym13040598.
31. GUPTA, V., SAXENA, P. and RUAN, D. Impact of Fibre Orientation and Volume Fraction on the Mechanical Properties of 3D-Printed Continuous Carbon Fibre-Reinforced Polyamide Composites using Towpreg Coextrusion Technology. *Advanced Engineering Materials*, 2025, vol. 27, no. 20. pp. 2500404. ISSN 1438-1656. DOI 10.1002/adem.202500404.
32. CAI, H. and CHEN, Y. A Review of Print Heads for Fused Filament Fabrication of Continuous Carbon Fibre-Reinforced Composites. *Micromachines*, /4, 2024, vol. 15, no. 4. pp. 432. ISSN 2072-666X. DOI 10.3390/mi15040432.
33. SONG, Q., et al. Research on Void Dynamics during in Situ Consolidation of CF/High-Performance Thermoplastic Composite. *Polymers*, /1, 2022, vol. 14, no. 7. pp. 1401. ISSN 2073-4360. DOI 10.3390/polym14071401.
34. WANG, Xiaochong; LI, Guixing; ZIA, Ali Akmal; TIAN, Xiaoyong; CHEN, Yuan, et al. An in-situ impregnation model for additive manufacturing via co-extrusion of continuous fibre bundles: A rigorous methodology for determining optimal manufacturing parameters. *Composites Part A: Applied Science and Manufacturing*, vol. 199 (2025), pp. 109259. Available from: https://www.sciencedirect.com/science/article/pii/S1359835X25005536.
35. LIAMPAS, Stylianos; KLADOVASILAKIS, Nikolaos; TSONGAS, Konstantinos and PECHLIVANI, Eleftheria Maria. Recent Advances in Additive Manufacturing of Fibre-Reinforced Materials: A Comprehensive Review. *Applied Sciences*, vol. 14 (2024), no. 22, pp. 10100. Available from: https://www.mdpi.com/2076-3417/14/22/10100.
36. BEAUMONT, Kieran D.; KUBALAK, Joseph R. and WILLIAMS, Christopher B. Multi-axis material extrusion of continuous carbon fibre composites: tool design and mechanical characterization. *The International Journal of Advanced Manufacturing Technology*, vol. 138 (2025), no. 11, pp. 5285–5307. Available from: https://doi.org/10.1007/s00170-025-15749-8.
37. VERVILLE, Mathieu and THERRIAULT, Daniel. High-performance and geometrically complex parts via co-extrusion additive manufacturing of multi-scale continuous carbon fibre-reinforced thermoplastic composites. *Composites Part B: Engineering*, vol. 310 (2026), pp. 113179. Available from: https://www.sciencedirect.com/science/article/pii/S1359836825010959.
38. YANG, Yuan; YANG, Bo; CHANG, Zhengping; DUAN, Jihao and CHEN, Weihua. Research Status of and Prospects for 3D Printing for Continuous Fibre-Reinforced Thermoplastic Composites. *Polymers*, vol. 15 (2023), no. 17, pp. 3653. Available from: https://www.mdpi.com/2073-4360/15/17/3653.
39. WANG, Fuji; WANG, Gongshuo; WANG, Hongquan; FU, Rao; LEI, Yajing, et al. 3D Printing Technology for Short-continuous Carbon Fibre Synchronous Reinforced Thermoplastic Composites: A Comparison between Towpreg Extrusion and In Situ Impregnation Processes. *Chinese Journal of Mechanical Engineering: Additive Manufacturing Frontiers*, vol. 2 (2023),

no. 3, pp. 100092. Available from: https://www.sciencedirect.com/science/article/pii/S2772665723000314. [viewed Apr 3, 2026].

40. ZHI, Quan; LI, Dongsheng; ZHANG, Zhikun; FU, Long and ZHU, Weijun. High-content continuous carbon fibre reinforced multifunctional prepreg filaments suitable for direct 3D-printing. *Composites Communications*, vol. 44 (2023), pp. 101726. Available from: https://www.sciencedirect.com/science/article/pii/S2452213923002346.
41. YU, Liguo; CHEN, Ke; XUE, Ping; CUI, Yonghui and 贾明印, Mingyin. Impregnation modeling and preparation optimization of continuous glass fibre reinforced polylactic acid filament for 3D printing. *Polymer Composites*, vol. 42 (2021), pp. 5731–5742. Available from: https://www.researchgate.net/publication/353911329_Impregnation_modeling_and_preparation_optimization_of_continuous_glass_fibre_reinforced_polylactic_acid_filament_for_3D_printing.
42. ZHUO, Peng; LI, Shuguang; ASHCROFT, Ian A. and JONES, Ivor A. Continuous fibre composite 3D printing with pultruded carbon/PA6 commingled fibres: Processing and mechanical properties. *Composites Science and Technology*, vol. 221 (2022), pp. 109341. Available from: https://www.sciencedirect.com/science/article/pii/S0266353822000835.
43. SÜTCÜLER, Yunus Alp; BEX, Guy J. P.; STUPP, Cesar A.; KODAL, Mehmet; TEN CATE, A. Tessa, et al. Lab-scale manufacturing of thermoplastic matrix-continuous carbon fibre filaments for additive manufacturing: Melt impregnation, properties of the filaments and its printed composites. *Polymer Composites*, vol. 46 (2025), no. 5, pp. 4317–4331. Available from: https://doi.org/10.1002/pc.29241.
44. LIU, Tengfei; TIAN, Xiaoyong; ZHANG, Manyu; ABLIZ, Dilmurat; LI, Dichen, et al. Interfacial performance and fracture patterns of 3D printed continuous carbon fibre with sizing reinforced PA6 composites. *Composites Part A: Applied Science and Manufacturing*, vol. 114 (2018), pp. 368–376. Available from: https://www.sciencedirect.com/science/article/pii/S1359835X18303518.
45. TRAJKOVSKA PETKOSKA, Anka; SAMAKOSKI, Blagoja; SAMARDJIOSKA AZMANOSKA, Bisera and VELKOVSKA, Viktorija. Towpreg—An Advanced Composite Material with a Potential for Pressurized Hydrogen Storage Vessels. *Journal of Composites Science*, vol. 8 (2024), no. 9, pp. 374. Available from: https://www.mdpi.com/2504-477X/8/9/374.
46. OPRIȘ, Ocsana; MORMILE, Cristina; LUNG, Ildiko; STEGARESCU, Adina; SORAN, Maria-Loredana, et al. An Overview of Biopolymers for Drug Delivery Applications. *Applied Sciences*, vol. 14 (2024), no. 4, pp. 1383. Available from: https://www.mdpi.com/2076-3417/14/4/1383.
47. FLÓREZ, María; CAZÓN, Patricia and VÁZQUEZ, Manuel. Selected Biopolymers' Processing and Their Applications: A Review. *Polymers*, vol. 15 (2023), no. 3, pp. 641. Available from: https://www.mdpi.com/2073-4360/15/3/641.
48. NASER, Ahmed Z.; DEIAB, I. and DARRAS, Basil M. Poly(lactic acid) (PLA) and polyhydroxyalkanoates (PHAs), green alternatives to petroleum-based plastics: a review. *RSC Advances*, vol. 11, no. 28, pp. 17151–17196. Available from: https://pmc.ncbi.nlm.nih.gov/articles/PMC9033233/.
49. RONG, Liyuan; CHEN, Xianxiang; SHEN, Mingyue; YANG, Jun; QI, Xin, et al. The application of 3D printing technology on starch-based product: A review. *Trends in Food Science &*

Technology, vol. 134 (2023), pp. 149–161. Available from: https://www.sciencedirect.com/science/article/pii/S0924224423000663.

50. KOBAYASHI, Ayano; HARADA, Yoshiki and MITOMA, Yoshiharu. In situ degradation of biodegradable bio-based plastics in urban soil: Pilot study for PLA, PHB, PHBH, and Bio-PBS in central Tokyo, Japan. *Science of The Total Environment*, vol. 1025 (2026), pp. 181632. Available from: https://www.sciencedirect.com/science/article/pii/S0048969726002937.
51. Biopolymers in additive manufacturing*In: Additive Manufacturing of Biopolymers*, pp. 39–63Elsevier, 2023. Available from: https://www.sciencedirect.com/science/chapter/edited-volume/pii/B9780323951517000016.
52. ERASLAN, Kerim; AVERSA, Clizia; NOFAR, Mohammadreza; BARLETTA, Massimiliano; GISARIO, Annamaria, et al. Poly(3-hydroxybutyrate-*co*-3-hydroxyhexanoate) (PHBH): Synthesis, properties, and applications - A review. *European Polymer Journal*, vol. 167 (2022), pp. 111044. Available from: https://www.sciencedirect.com/science/article/pii/S0014305722000489.
53. MÁRMOL, Gonzalo; GAUSS, Christian and FANGUEIRO, Raul. Potential of Cellulose Microfibres for PHA and PLA Biopolymers Reinforcement. *Molecules*, vol. 25 (2020), pp. 4653. Available from: https://www.researchgate.net/publication/344622901_Potential_of_Cellulose_Microfibres_for_PHA_and_PLA_Biopolymers_Reinforcement.
54. PETOUSIS, Markos; DAVID, Constantine; SAGRIS, Dimitrios; NASIKAS, Nektarios K.; PAPADAKIS, Vassilis, et al. Reinforced PHA/CNC Biocomposites in Extrusion-Based Additive Manufacturing. *ACS Omega*, vol. 10 (2025), no. 32, pp. 36613–36630. Available from: https://doi.org/10.1021/acsomega.5c05743.
55. CHEN, Huaiyou; KLEMM, Sophie; DÖNITZ, Antonia G.; OU, Yating; SCHMIDT, Bertram, et al. Tailoring the Mechanical Properties of Fungal Mycelium Mats with Material Extrusion Additive Manufacturing of PHBH and PLA Biopolymers. *ACS Omega*, vol. 9 (2024), no. 50, pp. 49609–49617. Available from: https://doi.org/10.1021/acsomega.4c07661.
56. IVORRA, Juan; VERDU, Isabel; GIMENO, Octavio; SANCHEZ-NACHER, L.; BALART, R., et al. Manufacturing and Properties of Binary Blend from Bacterial Polyester Poly(3-hydroxybutyrate-co-3-hydroxyhexanoate) and Poly(caprolactone) with Improved Toughness. *Polymers*, vol. 12 (2020), pp. 1118. Available from: https://www.researchgate.net/publication/341395050_Manufacturing_and_Properties_of_Binary_Blend_from_Bacterial_Polyester_Poly3-hydroxybutyrate-co-3-hydroxyhexanoate_and_Polycaprolactone_with_Improved_Toughness.
57. ALIOTTA, Laura; SEGGIANI, Maurizia; LAZZERI, Andrea; GIGANTE, Vito and CINELLI, Patrizia. A Brief Review of Poly (Butylene Succinate) (PBS) and Its Main Copolymers: Synthesis, Blends, Composites, Biodegradability, and Applications. *Polymers*, vol. 14 (2022), no. 4, pp. 844. Available from: https://pmc.ncbi.nlm.nih.gov/articles/PMC8963078/.
58. WU, Shuyi; ZHANG, Yang; HAN, Jiarui; XIE, Zhining; XU, Jun, et al. Copolymerization with Polyether Segments Improves the Mechanical Properties of Biodegradable Polyesters. *ACS Omega*, vol. 2 (2017), pp. 2639–2648. Available from: https://www.researchgate.net/publication/317575849_Copolymerization_with_Polyether_Segments_Improves_the_Mechanical_Properties_of_Biodegradable_Polyesters.

59. TSCHICHOLD, Tobias; MÄDER, Gabriel and YILDIRIM, Selcuk. Characterization of PBS and PBAT biocomposites reinforced with rapeseed press cake: Influence of filler content and particle size. *Materials Today Communications*, vol. 47 (2025), pp. 113214. Available from: https://www.sciencedirect.com/science/article/pii/S235249282501726X.
60. ROCKET-FIBRES. Carbon Fibre. Online. [viewed Apr 2, 2026]. Available from: https://www.rocket-fibres.com/products/carbonfibre.
61. LEADING FIBREGLASS ROVING MANUFACTURER. 300 Tex E-Glass Fibreglass Yarn. Online. [viewed Apr 2, 2026]. Available from: https://www.tfcomposite.com/300tex-e-glass-fibreglass-yarn.
62. GUODUN ARMOR. 1414 Para Aramid Yarn. Online. [viewed Apr 2, 2026]. Available from: https://guodunarmor.com/product/1414-para-aramid-yarn/.
63. JAIN, Nishant; CZASNY, Mathias; BUTZMANN, Till; KOBER, Delf; KARL, David, et al. Additive manufacturing of continuous regenerated cellulose fibre reinforced polylactic acid composites using *in-situ* impregnation material extrusion technique. *Composites Part C: Open Access*, vol. 17 (2025), pp. 100594. Available from: https://www.sciencedirect.com/science/article/pii/S2666682025000386.
64. *Standard Test Methods for Properties of Continuous Filament Carbon and Graphite Fibre Tows.* Available from: https://store.astm.org/d4018-17.html.
65. JIANG, Q., TAKAYAMA, T. and NISHIOKA, A. Improving the Accuracy of the Evaluation Method for the Interfacial Shear Strength of Fibre-Reinforced Thermoplastic Polymers through the Short Beam Shear Test. *Polymers*, /1, 2024, vol. 16, no. 7. pp. 883. ISSN 2073-4360. DOI 10.3390/polym16070883.
66. THOMSON, J. and RUDEIROS-FERNÁNDEZ, J. Characterization of interfacial strength in natural fibre – polyolefin composites at different temperatures. *Composite Interfaces*, /1, 2022, vol. 29, no. 1. pp. 1-22. ISSN 1568-5543. DOI 10.1080/09276440.2021.1913901.
67. SØRENSEN, B.F. and LILHOLT, H. Fibre Pull-Out Test and Single Fibre Fragmentation Test - Analysis and Modelling. *IOP Conference Series: Materials Science and Engineering*, July 1, 2016, vol. 139, no. 1. pp. 012009. ISSN 1757-899X. DOI 10.1088/1757-899X/139/1/012009.
68. VIEL, Quentin; ESPOSITO, Antonella; SAITER, Jean-Marc; SANTULLI, Carlo and TURNER, Joseph A. Interfacial Characterization by Pull-Out Test of Bamboo Fibres Embedded in Poly(Lactic Acid). *Fibres*, vol. 6 (2018), no. 1, pp. 7. Available from: https://www.mdpi.com/2079-6439/6/1/7.
69. Engineering Resources, Data Sheets & Guides. HexTow® AS4 Carbon Fibre Datasheet, -01-28, 2026. Available from: https://www.hexcel.com/resources/. [viewed Apr 3, 2026].
70. *Standard Test Method for Tensile Properties of Polymer Matrix Composite Materials.* Available from: https://store.astm.org/d3039_d3039m-08.html. [viewed Apr 3, 2026].
71. *Standard Test Method for Flexural Properties of Polymer Matrix Composite Materials.* Available from: https://store.astm.org/d7264_d7264m-21.html. [viewed Apr 3, 2026].
72. SAFWAT, Engie M.; KHATER, Ahmad G. A.; ABD-ELSATAR, Ahmed G. and KHATER, Gamal A. Glass fibre-reinforced composites in dentistry. *Bulletin of the National Research Centre*, vol. 45 (2021), no. 1, pp. 190. Available from: https://doi.org/10.1186/s42269-021-00650-7.
73. ELKOLALI, Moustafa; NOGUEIRA, Liebert Parreiras; RØNNING, Per Ola and ALCOCER, Alex. Void Content Determination of Carbon Fibre Reinforced Polymers: A Comparison between

Destructive and Non-Destructive Methods. *Polymers*, vol. 14 (2022), no. 6, pp. 1212. Available from: https://www.mdpi.com/2073-4360/14/6/1212.

74. *Standard Test Methods for Constituent Content of Composite Materials*. Available from: https://store.astm.org/d3171-22.html.
75. *Standard Test Methods for Void Content of Reinforced Plastics*. Available from: https://store.astm.org/d2734-16.html.
76. ANODAS. Micro Swiss Direct Drive Extruder with hotend for ExoSlide System. Online. [viewed Apr 16, 2026]. Available from: https://www.anodas.lt/en/micro-swiss-direct-drive-extruder-with-hotend-for-exoslide-system.
77. LEMONA. Joy-iT NEMA 17-02 Stepper motor. Online. [viewed Apr 16, 2026]. Available from: https://www.lemona.lt/joy-it-nema-17-02-stepper-motor.html.
78. FIBREMAX. Carbon fibre 3K, 1.8 kg, 5 km. Online. [viewed Apr 16, 2026]. Available from: https://www.fibremax.eu/carbon-fabrics/carbon-yarns/carbon-yarns-show-all/carbon-tow-3k-1-kg-5-km.html.
79. EBAY. 1414 Aramid Fibre tow Filament Yarn. Online. [viewed Apr 16, 2026]. Available from: https://www.ebay.com/itm/388068337457?var=655284889993.
80. HELIANPOLYMERS. BP330-05 PHBH Pellets. Online. [viewed Apr 16, 2026]. Available from: https://shop.helianpolymers.com/products/bp330-05-phbh-pellets.
81. POLYMERVERSE. PBS Powder Polybutylene Succinate Polybutylene Succinate Polymer Universal Fully Biodegradable Resin. Online. [viewed Apr 16, 2026]. Available from: https://www.polymerverse.com/collections/pbs/products/pbs-powder.
82. POLARFILAMENT. Biodegradable Natural PHA. Online. [viewed Apr 16, 2026]. Available from: https://polarfilament.com/products/biodegradable-natural-pha-1kg-1-75mm.
83. 3DPRINTERUNIVERSE. Geetech Mecreator 2 Desktop 3D Printer. Online. [viewed Apr 16, 2026]. Available from: https://3dprinteruniverse.com/products/geeetech-mecreator-2-desktop-3d-printer?variant=25243289287.